Sustainable materials for 3D concrete printing

Bhattacherjee, Shantanu; Basavaraj, Anusha S.; Rahul, A. V.; Santhanam, Manu; Gettu, Ravindra; Schlangen, Erik; Chen, Yu; Copuroglu, Oguzhan; Wang, Li; More Authors

Citation (APA)
Bhattacherjee, S., Basavaraj, A. S., Rahul, A. V., Santhanam, M., Gettu, R., Schlangen, E., Chen, Y., Copuroglu, O., Wang, L., & More Authors (2021). Sustainable materials for 3D concrete printing. *Cement and Concrete Composites*, *122*, Article 104156. https://doi.org/10.1016/j.cemconcomp.2021.104156

Important note
To cite this publication, please use the final published version (if applicable).
Please check the document version above.

Sustainable materials for 3D concrete printing

Shantanu Bhattacherjee [a], Anusha S. Basavaraj [a], A.V. Rahul [b], Manu Santhanam [a,*],
Ravindra Gettu [a], Biranchi Panda [c], Erik Schlangen [d], Yu Chen [d], Oguzhan Copuroglu [d],
Guowei Ma [e], Li Wang [e], Mirza Abdul Basit Beigh [f], Viktor Mechtcherine [f]

[a] *Indian Institute of Technology Madras, India*
[b] *Ghent University, Belgium*
[c] *Indian Institute of Technology Guwahati, India*
[d] *Delft University of Technology, Netherlands*
[e] *Hebei University of Technology, China*
[f] *TU Dresden, Germany*

ARTICLE INFO

ABSTRACT

This paper explores the sustainability aspects of binders used in concrete 3D concrete printing. Firstly, a prospective approach to conduct sustainability-assessment based on the life cycle of 3D printed structures is presented, which also highlights the importance of considering the functional requirements of the mixes used for 3D printing. The potential of the material production phase is emphasized to enhance the sustainability potential of 3DCP by reducing the embodied impacts. The literature on the different binder systems used for producing 3D printable mixtures is reviewed. This review includes binders based on portland cement and supplementary cementing materials (SCMs) such as fly ash, silica-fume and slag. Also, alternative binders such as geopolymer, calcium sulfo-aluminate cement (CSA), limestone calcined clay cement (LC3) and reactive magnesium oxide systems are explored. Finally, sustainability assessment by quantifying the environmental impacts in terms of energy consumed and CO_2 emissions of mixtures is illustrated with different binder systems. This paper underlines the effect of using SCMs and alternative binder systems for improving the sustainability of 3D printed structures.

1. Introduction

3D concrete printing (3DCP) has moved from being a laboratory technology to pilot projects involving multiple functional units. From successful applications in post-tensioned segmental bridges [1,2] to the restoration of buildings with architecturally efficient facades [3], printing with concrete has opened up many interesting opportunities. Digital construction could also be an answer for customizable mass housing units, suggesting that it is not a technology that is only intended for economically-developed countries.

The geometric and design flexibility afforded by 3D printing makes it possible to produce structural elements that are difficult to conceive with conventional formwork-based construction. This, coupled with structural optimization [4,5], could lead to massive benefits in terms of reducing the wastage of construction material. Additionally, the absence of formwork also implies associated savings in time and cost, which can

present many opportunities in both small- and large-scale projects. Furthermore, 3DCP technologies promise a pronounced increase in productivity, higher safety in precast plants and onsite construction, and more attractive jobs in the construction industry. For many regions of the world, the automation and digitization in construction might also efficiently mitigate the shortage of skilled labor. It is, however, important to bring in the perspective of sustainability to make a rational choice of 3D concrete printing methodology and assess where it could be more beneficial than conventional construction. The limited analyses of the sustainability of 3DCP in the literature substantiate the potential, especially for complex elements [6].

Sustainability is a broad term that goes much beyond the reduction of raw material usage and environmental impact. The treatment of sustainability in terms of the three pillars of economic, environmental and societal impacts has become universally accepted, with procedures to quantify the impacts. The most feasible to quantify are the economic
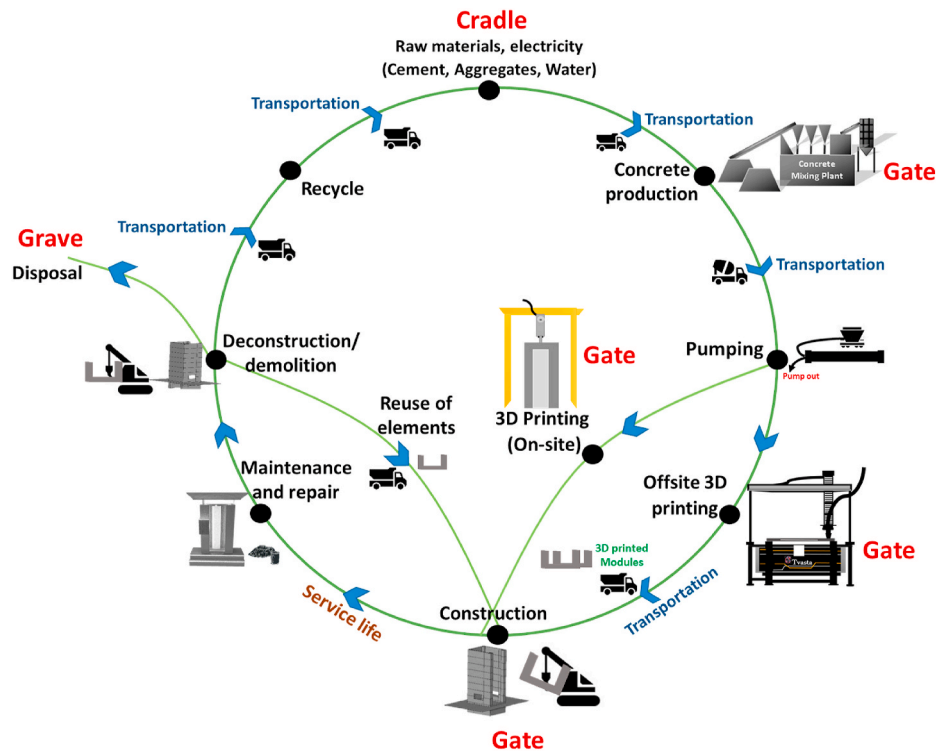

Fig. 1. A schematic sketch of the life cycle of a 3D printed structure.

consequences, especially in the context of construction, and the most complicated are the societal implications. When 3DCP is compared with conventional construction, savings in cost are expected due to the elimination of formwork and labour, and lower project durations. On the other hand, mixtures using unconventional ingredients, and stricter control of the proportions and the properties of the mix may increase the cost of the concrete. The environmental impact would be lowered by the elimination of formwork and reduction in material wastage but may increase if the binder content is very high. The positive societal impact of using 3DCP in the prefabrication plant and construction site is expected to be significant due to the reduction of manual labour for the lifting of formwork, and pouring and compaction of concrete, the employment of skilled operators for the printers (in semi-automated cases), and the reduction of errors and accident rates due to automation. Such aspects could also contribute to the 17 Sustainable Development Goals (SDGs) identified by the United Nations to drive action for the 2030 Agenda (https://sdgs.un.org/goals). Some goals and indicators directly influenced by the construction technology include [7] the upgradation of infrastructure with better technologies and processes reflected by lower carbon emissions (Target 9.4), ensuring safe and affordable housing (Target 11.1), and efficient use of natural resources in terms of per capita material usage (Target 12.2).

Comprising three parts, this paper presents an approach to assess the sustainability of 3D printing with emphasis on the carbon footprint and the energy demand, discusses the factors that could influence the outcomes of the assessment and illustrates an approach for the comparison of printable concretes with different compositions.

2. Sustainability assessment

The life cycle of the concrete/material used for 3D printing of concrete is given schematically in Fig. 1, considering all processes including the mining of raw materials used in cement and aggregate production, transportation of concrete and other materials, production of electricity, pumping of concrete, printing, construction, maintenance, and the end-of-life demolition or dismantling. Cognizance of all the relevant

processes is essential for assessing the potential of a given technology, considering different options and comparing with conventional construction. The first step in sustainability assessment is the definition or demarcation of the system boundaries. The different systems, which could be considered, can be classified as cradle-to-gate (ground-to-gate), gate-to-gate, cradle-to-grave and cradle-to-cradle, and the system boundaries are chosen to respond to the scope and purpose of the assessment. With reference to Fig. 1, various systems boundaries can be contemplated in the context of the sustainability assessment of 3D printing technology. The systems most relevant would be cradle-to-gate, which could cover the processes of (i) the mining up to the 3D printing in a factory, or (ii) the mining up to the completion of construction onsite. However, more reliable assessment (i.e., not requiring too much conjecture related to raw material sources and extraction methods) could be based on gate-to-gate systems, such as those that cover the processes employed in cement, aggregates and concrete plants up to the production of the 3D printed element in a factory or the completion of construction at the site. The cradle-to-grave system is obviously the most complete, though not very relevant since civil engineering structures are mostly designed to last several decades or even a few centuries making it practically impossible to speculate the processes that would be employed in the end-of-life stage for demolition, recycling and disposal. The ideal system, though unheard of in construction, would be cradle-to-cradle, where a new cycle would begin at the end of the previous one, such as the separation of all the concrete from the demolished structure into aggregates that can substitute pristine aggregates, and hydrated cement paste that can be used in cement manufacturing.

Fig. 1 also accommodates the different alternatives possible with the 3D printing technology. For example, the concrete could be made at the same place where the 3D printing is done or it could be procured ready-mixed, implying a gate in the cycle. Another example could be procurement of 3D printed modules from a prefabrication factory (i.e., a gate) with the assembly of the structure being done at the site instead of 3D printing it at the site.

In terms of the parameters to consider in the sustainability assessment, the most appropriate methodology would be to consider all the

Table 1
Designs for 3D printable mixtures.

Reference	Water to binder ratio	Cement	SCMs type and SCM/ Cement ratio	Chemical admixture	Remarks
Rahul and Santhanam [10]	0.32	1 (OPC 53)	Class F processed fly ash (0.25)	PCE based SP HPMC based VMA	Extrudability is characterised by measuring yield stress (using vane shear apparatus), flow value and extruding the mix through the printer. The concept of packing density was used to optimise the SP and VMA dosages of the mix to retain the cut-off yield stress. The probability of phase separation during printing was assessed using the concept of desorptivity (described in Ref. [19]).
Nerella et al. [37]	0.42 (water to cement ratio)	1 (CEM I 52.5R)	Fly ash (0.4) Micro-silica suspension with 50% solids content (0.42)	MCPF 5100 as SP	Developed the mixtures for the printing of a multi-storeyed apartment. The mixtures were prepared considering consistency retention over a long duration (measured using the Hagermann flow table), and rheological properties like high thixotropy (measured using the Haake Mars II rheometer). Pumpability was tested using sliding pipe rheometer.
Kruger et al. [38]	0.32	1 (CEM II 52.5 N)	Siliceous fly ash (0.28) Silica fume (0.143)	Modified polycarboxylate polymer as SP	Both dynamic and static yield stress were considered as important material properties
Ma et al. [11, 39]	0.27	1 (P.O 42.5R)	Fly ash (0.285) Silica fume (0.143)	Polycarboxylate-based SP	Considered the extrudability, buildability, open time, flowability (slump test, jumping table test, V-funnel test), structural build-up (cone penetration). Copper tailings were used as fine aggregates.
Chen et al. [40]	0.3	1 (CEM I 52.5R)	Low, medium, and high grade calcined clay, Limestone powder	SP VMA	Ram extrusion used to study the rheological behaviour. A good correlation found with Basterfield model. The medium grade calcined clay is reported to perform better than low grade and high grade clays considering the properties of buildability and printability.
Kazemian et al. [41]	0.43	1 (ASTM type II Portland cement)	Silica fume (0.11)	PCE based SP	A performance-based test protocol was developed to assess the fresh state properties of the printable mix. The properties considered are print quality, shape stability, and printability window. The print quality is considered satisfactory when the surface is free of defects, and layer edges are correctly distinguishable. Also, the dimensional conformity must be satisfied. Cylinder stability test was developed to measure the shape stability.
Le et al. [42]	0.28	1 (CEM I 52.5)	Fly ash (0.28) Silica fume (0.14)	Polycarboxylate based SP Retarder (amino-tris (methylenephosphonic acid), citric acid and formaldehyde)	The influence of retarder and accelerator is studied. Soil vane shear apparatus is used to assess the yield stress.
Gosselin et al. [43]	0.1 Water/ (cement+sand)	60–67% (CEM I 52.5 N)	Silica fume (17–20%) Limestone filler		Use of a 6-axis industrial robot.
Panda et al. [44]	0.45	1 (CEM 1)	Fly ash (.70)	Nanoclay	Printability was characterised by static yield stress, viscosity and thixotropy measurement.

SP – superplasticizer, VMA – viscosity modifying admixtures
Some mix also contains polypropylene fibers

relevant indicators, though this is quite complicated with the limited data available [7]. Considering the improvement of the sustainability of concrete as the goal of the assessment, it is justified to use broad measures such as decreasing the cement content, water requirement, cost, CO_2 emissions and global warming potential, and increasing the mechanical and durability performance. Many other earlier studies have taken the carbon footprint and embodied energy as principal indicators of sustainability, especially since other parameters vary with time and location (e.g., cost) or are not sensitive to the type of concrete being used (e.g., human or eco-toxicity). In line with this, comparisons can be made among elements or structural systems with the same performance, where the material can be expected to dominate the environmental impact as the contribution of the digital fabrication process itself is negligible [8,9]. Nevertheless, there could be some variations in the impacts due to the type of concrete mixer (i.e., pan-type or drum-type or concrete batch-type mixers, or continuous mixers) with implications in terms of energy consumption, useful life, consumables, etc. Similarly, the type of pump (i.e., piston- or screw-based [10,11] would also have an influence. The type of printer – gantry-based, robotic arm, and crane-based [12,13], as well as the scale, would affect the energy

consumption, though not considerably.

When sustainability assessment is made only for comparing different printable concrete mixtures, they should be of similar performance, defined in terms of the functional requirements of the printing process, which may be categorized as fresh state requirements (extrudability, buildability), hardened state requirements (inter-layer bond strength, flexural strength, cube compression strength etc.), and long-term performance requirements (resistance to chloride ingress, carbonation, and water ingress). The bond between the printed layers also plays a critical role in both the short- and long-term performance of the structure.

3. 3D printable mixtures based on conventional cementitious materials

3D concrete printing technology requires concrete with special characteristics. Such mixtures are designed based on three primary material parameters, namely pumpability, extrudability and buildability, which are basically the ability to be pumped, extruded and to sustain load of consecutive printed layers without failure, respectively [14–18]. The pumpability and extrudability are governed by the

Table 2
Details about aggregates used in 3D printed mixtures.

Paper	Aggregate to cement ratio	Fine aggregates properties	Remarks
Rahul and Santhanam [10]	1.87	Quartz sands are used as fine aggregates, ranging in size from 10 to 1000 μm.	Mixtures with 8 mm coarse aggregates are also printed
Nerella and Mechtcherine [37]	2.88	Three sand samples with size ranges from – 0.3–0.6 mm, 0–1 mm and 0–2 mm.	
Kruger et al. [38]	2.02	Continuously coarse graded local sand with 4.75 mm as maximum particle size.	
Ma et al. [11]	1.71	Sand and copper tailings are used as fine aggregates.	
Chen et al. [40]	1.5 (sand to binder) 3.75 (sand to cement)	Sand with maximum size of 2 mm.	
Mechtcherine et al. [68]	2.50 (aggregate to binder)	Max aggregate size of 8 mm with ranges of sand from 0.06 to 0.2 mm, 0–1 mm, 0–2 mm, 2–8 mm	Mixture successfully printed up to 10 layers with each layer 50 mm height

properties of consistency, cohesiveness, stability and probability of phase separation under the application of pressure [19–21]. The extrudability and pumpability are further governed by the rheological properties of the lubricating layer [22,23]. The basic parameters governing rheology of concrete are yield stress, viscosity and thixotropy [18,22,24,25]. The buildability of the 3D printable mixture is affected by parameters such as static shear yield stress, dynamic shear yield stress [26, 27], green strength and early age elastic modulus [28–30]. These parameters further evolve with time due to hydration of cement, and are affected by the curing conditions [31,32]. The other critical parameters for the 3D printing of concrete are the open time of workability, printability window, thixotropy open time, layer bond strength and printing time gap [14,18,33]. The layer bond strength (adhesion) depends on the printing time gap, layer geometry and environmental conditions affecting the surface properties (e.g., drying of surface) [34–36].

Some typical binder systems for 3D printable mixes are given in Table 1, along with the test protocols used to achieve the mix, and the details of the aggregate type and content used are presented in Table 2. It is seen that the use of supplementary cementitious materials (SCMs) and high dosages of superplasticizer are common in all the mixtures. Some mixtures also have polypropylene fibres and viscosity modifying agents. It should be noted that the development and optimization of the mixtures depend on the printer characteristics, as well as the requirements posed by the element or module to be printed.

Durability studies of 3D printed concrete have been performed by several authors. As the structures are printed in layers in this method of construction, the printing time gap and environmental conditions could affect the surface properties of the layers, and limit the durability. The microcracks formed at the layer due to shrinkage during the printing time gap could permit chloride penetration and water ingress, and in addition to that, the freeze-thaw cycling is seen to make the interlayer joints more vulnerable and affect the bond strength [45–49].

3.1. Influence of different types of SCMs

The incorporation of SCMs in 3D printable concrete could have significant consequences for its properties. In general, the early age strength is seen to be low, except when a low dosage of metakaolin was used. On the other hand, the microstructure is less porous due to the SCMs, leading to an increase in durability (e.g., fly ash and silica fume

can be used to improve resistance to chloride penetration) though carbonation is observed to increase. The extent of OPC replacement with SCMs is summarized in Table 1, which lists the binder compositions from some landmark studies on 3D printable concrete. Binary and ternary blended mixtures are used to increase the resistance to phase separation under pressure, along with optimized plastic viscosity and yield strength, and consequently improve the stability of the 3D printed concrete. Fly ash is beneficial in terms of workability [50], while silica fume is widely used in 3D printed concretes due to its ability to resist phase separation, increase yield stress and plastic viscosity [51–57]; additionally, the mechanical performance and impermeability in hardened state are improved [41]. The shape stability and robustness of fresh printing mixture is also improved on addition of silica fume [18,41]. Adding ultra-fine fly ash was found to be beneficial to the workability of 3D printable concrete by reducing yield stress and viscosity [58] at the early stage. The combination of cement, silica fume or micro-silica (well dispersed), fly ash, and fine sands lead to a high packing density, contributing to strength and rheological behaviour [37,39].

High volume substitution of fly ash and slag has been reported by Panda et al. [44,59] whereas Bentz et al. [60] and others [61,62] have used limestone in the binder. Though silica fume and slag provide benefits in terms of the enhancement of performance and reduction of the environmental impact, the availability of these materials worldwide is limited [61,63]. The amount of fly ash available is relatively higher but more than 66% of the available material is not suitable for blending with cement due to quality reasons [64]. Other sustainable alternatives have been suggested by Chen et al. [65] and Beigh et al. [66] based on combinations of limestone and calcined clay along with OPC. The effect of limestone calcined clay binder on the properties critical for concrete 3D printing is discussed in section 4.2.

This section highlights the influence of SCMs on material properties (workability, strength, and durability) and the sustainability of concrete. The replacement with fly ash or GGBS is advantageous in terms of environmental performance but the use of silica fume will make the concrete more expensive (as it is costlier than cement and other SCMs). The calculation of sustainability of 3D printable concrete with SCMs should consider functional parameters such as pumpability, extrudability and buildability, as they are facilitated by the use of silica fume and fly ash. It can be concluded from this section that judicious use of SCMs is necessary to design sustainable 3D printable mixes.

Workability is one of the important parameters for 3D printed concrete, and high dosages of superplasticizer are required due to use of low w/b ratios [67]. Apart from workability, phase separation is also an important parameter for pumpability and extrudability of concrete. Desorptivity has been used as a parameter for evaluation of phase separation by Ref. [19], and a decrease in desorptivity was observed with a decrease in w/c ratio.

Concrete requires a high amount of good quality (potable) water considering its bulk production and curing needs. Consequently, the ecology and economy are influenced by the consumption of fresh water in manufacturing of concrete. 3D printing can be used to print concrete with low water to binder ratio, leading to lower water demand. Additionally, the total material consumption can be reduced by structural optimization leading to further reduction in the water requirement.

3.2. Influence of aggregate content and type

The details about the aggregates used in studies on 3D printed concrete are reported in Table 2. The aggregates are diverse, including locally mined sand, copper tailings, quartz sand (maximum size of 2 mm). A few attempts to print mixtures with coarse aggregates have been reported: Rahul and Santhanam [10] printed mixtures with lightweight coarse aggregate of size up to 8 mm (30% of total aggregate content), and Mechtcherine et al. [68] printed 10 layers (height of 500 mm) with 8 mm coarse aggregates.

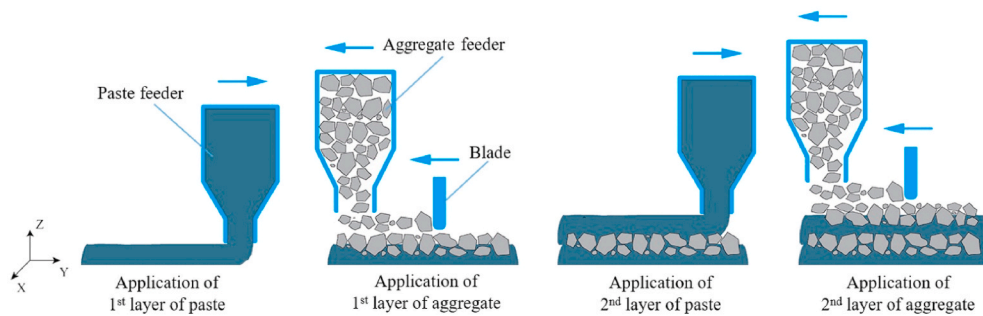While the studies on cement-based materials for 3D printing mainly

Fig. 2. 3D printing concrete with coarse aggregate by particle bed spreading method [77].

focus on the printability and mechanical properties of cement mortars [17,69,70], there are major deficiencies with respect to early shrinkage cracking, weak interlayers, the late realization of bearing capacity and long-term durability, etc., that could seriously restrict the application of this technology in practical applications [9,71,72] and affect the sustainability. Increase in coarse aggregate content leads to a considerable decrease in the hydration heat and shrinkage and improves volumetric stability of concrete [73]. Furthermore, the use of coarse aggregates is preferable because of the lower cost (economic feasibility/sustainability), and ecological sustainability due to considerably lower binder content, which is the major component responsible for energy consumption and CO_2 footprint in concrete production. Incorporating coarse aggregate into 3D printing cement-based materials is one of the important directions in the future research, especially for large-scale 3D printing [74].

Another aspect is that the use of coarse aggregates requires a larger cross-section of print filaments to accommodate larger particles. Such an increase in layer cross-section leads to the increase in concrete deposition rate, which is a product of layer cross-section and printhead speed, being a major parameter with respect to productivity, and thereby for economic sustainability. For example, for a printhead speed of 0.4 m/s, the deposition rate increases from 0.58 m^3/h to 10.8 m^3/h when the layer cross-section increases from 20 mm × 20 mm–150 mm × 50 mm [75].

In this context, the use of coarse aggregates also helps achieve higher values of static yield stress, which in turn helps attain better shape stability of the deposited filaments and high buildability of the print element. Larger filament cross-sections with considerable layer height require high shape stability. Ivanova and Mechtcherine [76] observed that not only the initial static yield stress increased with the increasing coarse aggregate content but also the rate of its development with time.

However, Mechtcherine et al. [68] reported that due to the presence of coarse aggregates in concrete, both processing the concrete, especially at the printhead, and testing its rheological properties relevant for 3D-printing become more challenging in comparison to mortar or paste. Printing with concrete containing coarse aggregates results in more ambitious demands on the concrete conveyor and on the shaping tools of the printhead in respect of delivery rates, robustness, and resistance to wear [9,68]. Yu et al. [77] proposed a particle bed printing method for binding coarse aggregate where gravels with the particle size range of 1.18–7 mm were evenly spread between the cement-based material layers (Fig. 2), and the maximum aggregate content could reach 40%.

Additionally, the sustainability of concrete depends on the type of aggregate. While production of gravel is usually less energy-intensive compared to sand [78], natural aggregates require less energy for their production than artificially produced aggregates. However, in some regions gravel has becomes rare or completely unavailable leading to local production of artificial aggregates as a sustainable solution. Recycled aggregates perform better in terms of environmental sustainability and fulfil the sustainable development goals [7], providing for similar economic and social performance.

Particle packing is used by several authors to reduce the amount of binder, to optimise the w/b ratio and to reduce the drying shrinkage [79–81]. For a given paste volume, an increase in aggregate packing density can improve workability, which is due to the increase in the excess paste thickness surrounding the aggregate particles [10,37, 82–84]. The concept of particle packing has been used to decrease the binder content, with better performance in terms of sustainability (reduction of CO_2 equivalent emission by 34% and material cost by 6.24%) by several authors [46,84]. 3D printable mixes have also been designed by optimising the dry ingredients using the particle packing method [18]. Apart from the conventionally used aggregate, some eco-friendly aggregates can also be adopted in the manufacturing of 3D printing material, such as recycled concrete aggregate, recycled glass [85,86], ceramsite particles made by river sediment, etc. The mixture with recycled aggregate designed on the principle of particle packing method showed better sustainability potential than a conventionally designed mix [87].

Additionally, the PSD can affect the specific surface area (SSA) of the granular skeleton that needs to be coated with cement paste. A higher SSA of the granular skeleton can result in a reduction in the paste film thickness surrounding the solid particles, thus leading to lower workability or higher water/admixture demand [88,89]. For a given volumetric composition of blended cement, the SSA and PSD of cementitious materials can have a substantial effect on heat evolution, microstructure, and hardened characteristics of cement-based materials [90–93].

4. Alternative material systems for 3D printing

4.1. Geopolymeric binders

Geopolymer and alkali-activated materials are gaining popularity as sustainable mixes for use in 3D concrete printing. The advantage of printing geopolymer lies in the rapid hardening nature of the mixes, which can significantly improve the buildability without the need of any additional chemical accelerators. Literature reveals that the binder selection of printable geopolymers, such as FA, slag etc. can significantly affect the fresh properties including the dosage of different alkali activators. According to Panda et al. [94], compared to fly ash, ultrafine slag addition increased the static yield stress and viscosity of materials due to angular shape of slag (interlocking effects), which in turn improved the buildability of the 3D structures. However, the dosage of slag was recommended to be carefully controlled since the addition of slag decreased the setting time while limiting the open time. In another study, Alghamdi et al. [95] investigated rheological properties of sodium-alkali-activated FA-based material and found replacing FA with limestone significantly decreased shear yield stress and viscosity. They concluded that adding limestone could improve the material printability due to higher spread diameter in slump test and lower viscosity. Rheological properties of geopolymer concrete are initially governed by the viscosity of activators and later by the formation of cross-linked polymers as the result of polycondensation reaction. Panda et al. [96]
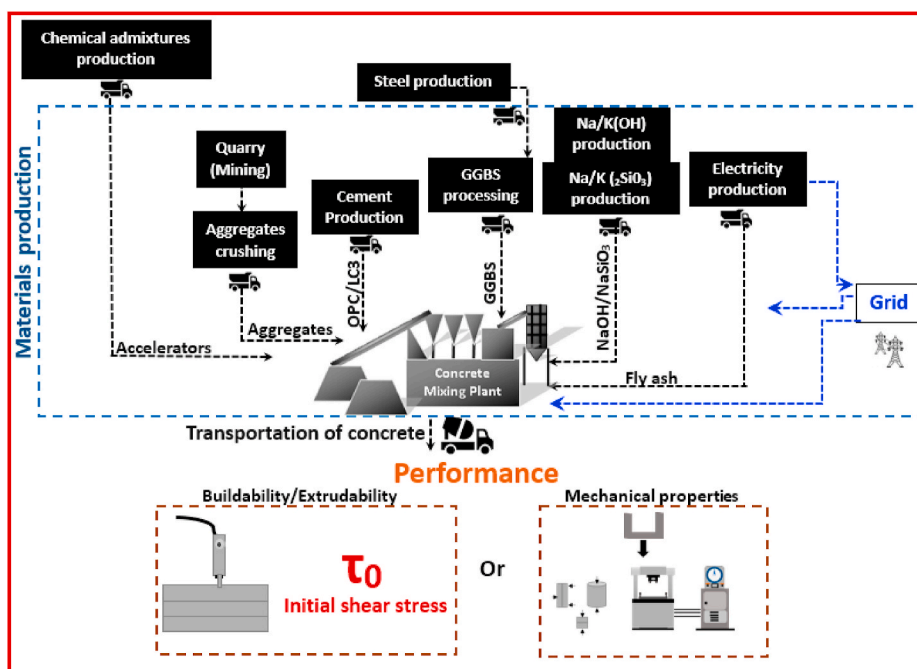
Fig. 3. System boundaries considered for the sustainability assessment.

Table 3
Impacts associated with the binders used in the study.

Binder/ Material	kg CO_2/ kg	MJ/kg	Reference
OPC	0.91	5.9	Gettu et al. [170]
GGBS	0.07	1.03	Gettu et al. [170]
Fly ash	0	0	
Silica fume	0	0	
LC2	0.248	3.3	Gettu et al. [176]
NaOH	1.3586	20.7	Kumar et al. [177] Ecoinvent database [172, 178]
Na_2SiO_3	0.762	10.8	Kumar et al. [177] Ecoinvent database [172, 178]
CSA	0.6	1.2 (Theoretical energy)	Hanein et al. [179]

conducted investigations on the effects of MR and activator solution-to-binder ratio on the rheology of geopolymer material. With a water-to-solid (w/s) ratio of 0.3, increasing MR from 1.8 to 2 resulted in a significant increase in both static yield stress and viscosity, which was explained by a higher activator viscosity with the increasing MR. However, when w/s increased to 0.35, both yield stress and viscosity experienced a substantial decrease and the increase in MR had minor positive effects on these rheology properties. It is recommended that the activator solution-to-binder ratio could be a proper proportioning parameter for practical applications [96], hence this ratio should be carefully designed and monitored for geopolymer 3D printing. In the research by Bong et al., the performance of Na-based activator was compared with K-based activator in terms of workability and shape retention of geopolymer for 3D printing [97,98]. Under similar conditions, Na-based activator resulted in positive effects on the flowability of fresh geopolymer compared with K-based activator. This result can be attributed to the difference of alkaline solution viscosity which finally affected the geopolymer viscosity. Researchers also have used one-part geopolymer mortar for 3D printing application due to transport and handling issues associated with liquid-based silicate activators [94,99]. The fresh properties of one-part 3D printable mortar were found to be

better than the liquid-based geopolymer due to difference in reaction medium viscosity.

Panda et al. [100] investigated the effects of slag and SF replacement on the structure build-up rate of FA-based geopolymer. It was found that 10% slag outweighed 10% SF in terms of improving yield strength development in 10–30 min after mixing, which is attributed to rapid hardening of the material due to presence of Ca containing SCMs. Besides, both SF and slag are found to promote the thixotropy of geopolymer due to the higher value of the thixotropic index obtained from the structural breakdown test. In a recent study, Muthukrishnan et al. [101] attempted to improve the structural build-up of geopolymer by microwave heating. The results demonstrated the introduction of a new print head mechanism to produce set-on demand concrete for 3D printing application.

Regardless of the binder type, the fresh properties of geopolymer concrete can be tailored by the addition of different types of additives. The main additive supplemented to printable geopolymers and alkali-activated binders is nanoclay, as reported in Ref. [102]. Apart from nanoclay, other additives such as sodium carboxymethyl starch (CMS) and hydromagnesite seeds have also been incorporated into geopolymer mixtures and investigated. According to Sun et al. [103], the addition of CMS promoted both yield stress and viscosity at different rates, which could reduce the risk of segregation whilst avoiding filament collapse. However, the porosity of printed filaments increased with an increase in CMS dosage leading to weak internal structures and lower strength. On the other hand, the addition of 1%–2% hydromagnesite seeds was found to exhibit minor influence on the rheological properties of the alkali-activated slag binders [102]. Different types of fibres are also incorporated in the printable geopolymer to improve the ductility; the resultant effects on rheological behaviour have been investigated by many researchers [104]. Al-Qutaifi et al. [105] characterized the effect of steel fibres and polypropylene (PP) fibres on the geopolymer workability via relative slump value. They found that the addition of 0.5% PP fibres had more negative effects on the flowability compared with that of 1.0% steel fibres, due to the significantly lower relative slump value by PP fibres. In another study, a negative correlation was found between PP fibre dosage and workability, indicating an increased risk of blockage during pumping of geopolymer mixes.
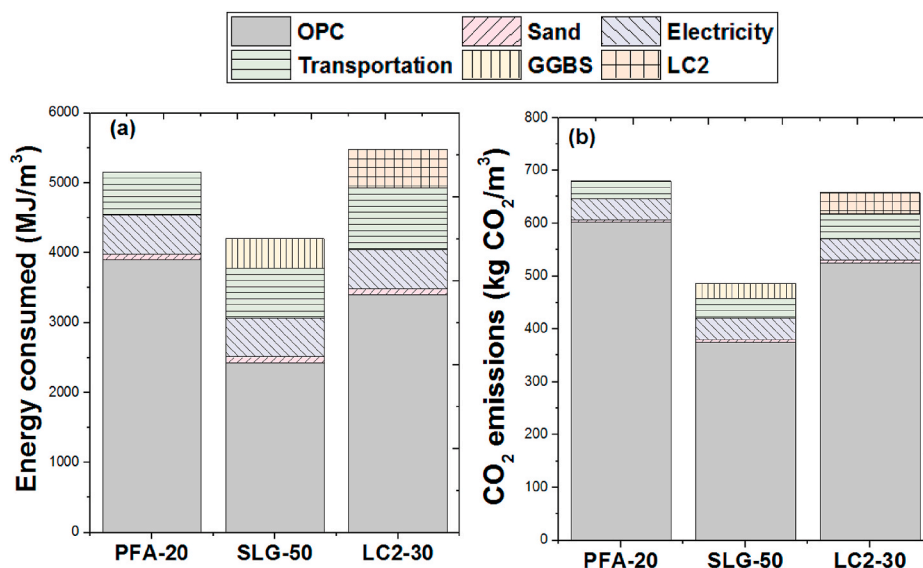
Fig. 4. Environmental impacts of concrete mixes used for 3D printing, all with 1.6 kPa initial yield stress.

4.2. Composite cementitious systems including limestone-calcined clay cement (LC3)

The conventional SCMs, including fly ash, blast-furnace slag, and silica fume, may not be available everywhere for continued long-term usage [61]. The total amounts available of slag and silica fume limited, and the supply chain of fly ash is threatened by the retirement or elimination of coal-fired power plants in many countries, e.g., the United States, the United Kingdom, and the Netherlands [106]. Finding alternative SCMs appears to be an urgent issue to ensure uninterrupted use of sustainable cementitious materials. Compared to the common SCMs, limestone, and (calcined) clay stand out as ideal raw material candidates that are largely abundant worldwide [61].

Limestone powder is commonly utilized as a filler component in the binder. The effect of limestone powder on rheology is primarily dependent on the physical characteristics of particles, e.g., fineness and surface roughness [107]. For improving the workability of fresh cementitious materials, a proper amount of limestone with a similar or coarser particle size compared to that of portland cement can be added into the mixture [108]. In contrast, the workability of fresh mixtures can be reduced by using an ultrafine limestone, which may be due to the enhancement of inner particle friction and the high adsorption of water and superplasticizer [109]. Filler effect is believed as the primary influence of limestone on cement hydration. Replacing a small content of portland cement by limestone could accelerate the early age hydration due to the increase of nucleation sites provided by the surface of the limestone particle [110]. In contrast, if the substitution of portland cement by limestone alone is higher than 10% by mass of binder, the mechanical performance of hardened cementitious materials can be strongly affected, which is attributed to the dilution effect [61,62].

Using calcined clay as a portland cement substitute could bring many benefits to 3DCP. Arguably, the most important aspect is the abundance of accessible clay reserves. Kaolinitic clay, being technically most suitable, is rich in tropical and subtropical environments, i.e., in India and Southeast Asia [111]. Another advantage is that the burning temperature for producing calcined kaolinitic clay is 700–850 °C, which is considerably lower than that of portland cement clinker production (1250–1450 °C) [61,112]. According to Huang et al. [113], producing 1 kg of calcined clay only emits 0.25–0.37 kg of CO_2 (about 1 kg of CO_2 in the case of Portland cement). Third, the ternary blend of limestone, calcined clay, and clinker (LC3) has been developed and studied by many researchers. LC3-50 cement (15% limestone, 30% calcined clay,

50% clinker, and 5% gypsum), as the most typical one, have been successfully manufactured during industry trials in Cuba and India [61,114, 115]. Metakaolin that can be regarded as the main reactive phase (comprises reactive aluminate and silicate) in calcined clay could react with calcium hydroxide forming C-(A)-S-H. Studies [116,117] have shown that utilizing calcined low-grade kaolinitic clay (about 40% of metakaolin) in LC3-50 binder could produce comparable compressive strength with plain cement from 7 days. Low-grade kaolinitic clays are inexpensive and may be acquired from quarries of cement plants [61]. Finally, except for the pozzolanic reaction induced by metakaolin, the calcite from limestone could react with alumina species in the pore solution for forming AFm phases (calcium hemi- and monocarboaluminate phases), which stabilizes the early formed ettringite [61,112,118]. All these reactions could contribute to the refinement of the capillary pores in the hardened cementitious materials. Recent results showed that using LC3 binder could also improve the durability of hardened concrete, i.e., excellent resistance of sulfate [119] and chloride attacks [120–123], and mitigation of alkali-silica reaction [61,124].

Chen et al. [40] investigated the possibilities to develop limestone-calcined clay-based cementitious materials for 3D concrete printing. Their results showed that the effect of calcined clay addition on the rheology of fresh mixtures is critical during the printing operation. The workability of fresh cementitious materials is generally reduced by the addition of calcined clay [108,125]. Because of the relatively low fineness, high specific surface area and layered structure of calcined clays, large quantities of water and superplasticizer are required in the blended mixtures [126–129]. According to Refs. [40,130,131] adding a proper amount of calcined clay in the mixture could enhance the buildability and structural build-up behavior. However, such influences on the fresh properties of cementitious materials may vary depending on the type of calcined clays used. For example, Chen et al. [132] found that increasing the metakaolin content in calcined clay can reduce the initial setting time and increase the green strength (within the first 4 h after mixing) of fresh mortars. As reported by Aramburo et al. [133], calcined clay with a high reactive aluminate amount could enhance the structuration rate of fresh pastes. Beigh et al. [66] stated that the presence of uncalcined kaolinitic clay seems to influence the structural build-up behavior of LC3 pastes.

Besides, it must be noted that the calcined clay may contain many impurities, such as uncalcined kaolinite, muscovite and montmorillonite. PCEs-based superplasticizers can be significantly adsorbed on swelling clays, especially montmorillonite. The presence of swelling
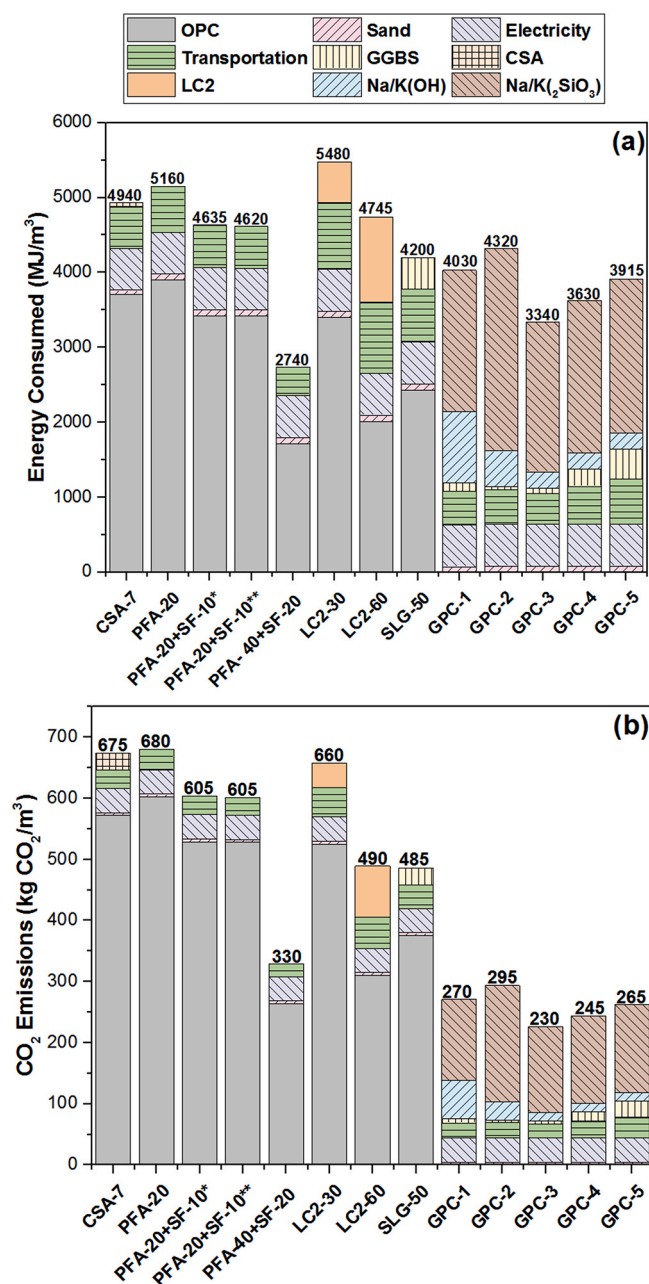
Fig. 5. Environmental impact (of printable concrete mixes) with different binders.

clays strongly affects or even nullifies the dispersion of such PCEs [134, 135]. As of today, the development and implementation of limestone-calcined clay-based binders in the context of extrusion-based 3D concrete printing is still in progress. Further investigation into these binders could reveal their high potential to be strong candidates for sustainable and low-cost constructions in the near future.

4.3. CSA cement

An environment-friendly alternative to ordinary portland cement (OPC) is the use of calcium sulphoaluminate cement. Compared to OPC, about 49% lower CO_2 emissions occur during its production [136–138]. The CSA clinker production happens at a temperature of 1250 °C, which is 200 °C lower than that required for producing OPC and hence, lesser burning of fossil fuels. Also, CSA clinkers formed at a lower temperature are much easier to grind, resulting in further energy savings [139].

Table 4
Calculated environmental impacts and performance criteria considered.

Particulars	3D printing mixes with OPC + conventional SCMs				Alternative binders								
	OPC+ 20% PFA [19]	OPC +20% PFA+10% SF* [42]	OPC +20% PFA+10% SF** [38]	OPC +40% PFA+20%SF [180]	OPC+ 50% SLG [19]	OPC+ 30% LC2 [19]	OPC+ 60% LC2 [40]	Geo-Polymer Concrete GPC-1 [14]	GPC- 2 [180]	GPC-3 [181]	GPC-4 [181]	GPC-5 [181]	OPC+ 7% CSA [142]
CO_2 emissions (kgCO_2/m^3)	680	605	605	330	485	660	490	270	295	230	245	265	675
Energy consumed (MJ/m^3)	5150	4635	4620	2740	4200	5480	4745	4030	4320	3340	3630	3915	4940
Shear Yield stress (kPa)	1.6	0.55	2.95	13.8	1.60	1.60	7.5-11.0	0.80	13.52	0.23 Nm (Torque)	0.30 Nm (Torque)	0.18 Nm (Torque)	2.73
Shear measurement	Vane shear apparatus	Vane shear apparatus	ICAR plus rheometer	Viscomat and calibration curve	Vane shear apparatus	Vane shear apparatus	Ram extrusion test and Basterfiled et al. model	Rotational rheometer with vane	Viscomat and calibration curve	RMB-2 rotational rheometer with a helix impeller			Penetration test
kgCO_2/kg of binder	0.81	0.73	0.72	0.46	0.59	0.80	0.72	0.35	0.38	0.30	0.32	0.34	1.00
MJ/kg of binder	6.25	5.60	5.58	3.84	5.10	6.70	6.2	5.20	5.66	4.45	4.77	5.08	7.30

Ratio of binders (PFA: SLG: SF) used in GPC mixes: 1) GPC-1 = 0.78:0.13:0.076 2) GPC-2 = 0.84:0.05:0.1 3) GPC-3 = 0.9:0.1:0 4) GPC-4 = 0.7:0.3:0.5) GPC-5 = 0.5:0.5:0

The primary phase in CSA cement is Klein's salt or Ye'elimite (50–80%). The early hydration of CSA cement occurs quite rapidly due to the fast hydration of Ye'elimite in the presence of gypsum to form ettringite [140,141]. A few researchers have partly replaced OPC with CSA cement to enhance the buildability of 3D printable mixtures [142, 143]. For instance, Khalil et al. [142] examined the buildability of a mixture containing 7% replacement of OPC with CSA cement. The buildability was assessed based on the numbers of layers that could be printed using a silicon gun. It was observed that the mixtures containing CSA cement showed much higher buildability. The authors also noted a faster evolution of yield stress with time for the mixture containing CSA cement. Recently, Manu et al. [144] developed a printable concrete formulation containing 100% CSA cement. To increase the open time required for smooth pumping, they investigated the use of retarders such as borax and gluconate. The addition of gluconate was found to increase the open time but significantly influenced the compressive strength development at early ages. However, the addition of borax increased the open time without adversely affecting the compressive strength development. Similarly, Chen et al. [145] studied the influence of tartaric acid on the setting behaviour of 3D printable CSA cement. The addition of tartaric acid increased the setting time without influencing the 1-day compressive strength.

Unlike OPC cement that undergoes an overall volumetric shrinkage upon its reaction with water, the hydration reaction of CSA cements results in a overall volume expansion. Since 3D printed concrete elements are more prone to shrinkage due to the lack of formwork and the high binder content [146], the design of shrinkage compensating binder systems is another domain where CSA can find application [147–149].

There are only limited studies on the rheological behaviour of CSA cement. Ke et al. [150] compared the rheological behaviour of CSA cement and OPC having the same water-cement ratio. The CSA cement showed a much higher plastic viscosity and exhibited a shear thickening behaviour. Chen et al. [151] studied the evolution of yield stress and thixotropy of 3D printable CSA mixtures containing metakaolin as a rheology modifier. The thixotropy was investigated based on the loop area obtained from the ramp-up and ramp-down of shear rate. The authors observed that the addition of metakaolin led to a more rapid evolution of yield stress and increased the loop area in the ramp-up ramp-down test.

For use in large-scale 3D printer systems, an aspect that requires attention is the pumping behaviour of concrete with CSA cement. Manu et al. [144] studied the rheological properties of the lubricating layer formed during pumping of CSA-based printable concrete using the tribometer approach [152]. They observed that although the lubricating layer properties were similar to those of OPC mixtures, the CSA mixture exhibited a higher pumping pressure due to the high plastic viscosity of the bulk concrete. The partial substitution of CSA with limestone (10–30%) was found to reduce the plastic viscosity of the bulk concrete and lower the required pumping pressure.

Despite the environmental benefits and its many other advantages, the use of CSA cement has been fairly limited in the construction industry. This can be mainly attributed to its much higher cost than OPC since its production requires the expensive mineral, bauxite [138]. In this regard, the use of cement with intermediate Ye'elimite content (20–30%), such as the calcium sulphoaluminate belite (CSAB) cement, is recently gaining popularity [153,154]. Since this cement requires lesser bauxite content for its manufacture, the cost of CSAB is comparable to that of OPC. With further research and development of CSAB cement, it can be a more cost-effective, at the same time, environmental-friendly option to replace OPC cement for large-scale projects.

4.4. Reactive magnesium oxide cement

Reactive magnesium oxide cement (RMC) (also known as reactive magnesia or caustic-calcined magnesite) is primarily produced from the calcination of magnesite, while a smaller fraction is also produced by converting the chloride and sulfate of magnesium present in seawater to $Mg(OH)_2$, and then subsequently calcining it to obtain MgO [155,156]. From a sustainability point of view, its use has several advantages. Firstly, its calcination temperature is in the range of 650–800 °C, which is much lower than OPC [155,156]. Another advantage is its ability to sequester carbon dioxide from the atmosphere during its curing process [157–160]. When mixed with water, it converts to $Mg(OH)_2$ and then carbonates to form hydrated magnesium carbonates (HMCs), resulting in strength development. Finally, the HMCs can be calcined to obtain back the reactive MgO, providing potential for complete recyclability [161].

Recently, Khalil et al. [162] examined the prospects of using RMC in additive manufacturing using a small syringe-based 3D printer. In their study, the printability of a pure RMC paste was evaluated. The initial mixture had poor buildability; however, the addition of a small amount (3%) of highly reactive caustic MgO was found to significantly enhance the buildability. Even though both the RMC and caustic MgO additive had a similar chemical composition, the caustic MgO had much higher reactivity due to its lower crystallinity and higher specific surface area. Its addition provided more active nucleation sites, increasing the rate of hydration of RMC. The authors also investigated the compressive strength and the microstructure of the printed and cast samples made using the RMC after three days of ambient curing and seven days of carbonation in an environmental chamber. The printed elements showed higher compressive strength and also a denser concentration of HMCs. The authors attribute the higher degree of carbonation to the higher uptake of CO_2 through the interlayers present in the printed elements.

Even though the work by Khalil et al. [162] is promising, there are many barriers to be overcome before RMC can be successfully implemented in large-scale 3D printing projects. First, the current methods of manufacturing RMC are cost-intensive. Second, most of the early studies on RMC were focused on hydration and carbonation characteristics [158,159,163,164], and there is minimal understanding on the rheology, early age reaction kinetics and pumping behaviour of RMC. Knowledge of these aspects is critical for RMC to be used in 3D printing projects.

Finally, some variants of RMC have also been developed in recent times. For instance, magnesium phosphate cement (MPC) can be obtained as a result of the reaction between MgO and acid phosphate salts [165]. Weng et al. [166] examined the feasibility of one type of this variant, magnesium potassium phosphate cement, in 3D printing using a small-scale printer. To modify the setting behaviour and increase the open time, fly ash was used as an additive, while silica fume was added to enhance the rheological and mechanical characteristics. Even though MPC could be successfully implemented in this study, it must be also pointed out that there are similar issues such as the high production cost and the lack of research focusing on fresh and early age behaviour of MPC. In summary, RMC and its variants like MPC have considerable benefits in terms of reducing CO_2 emissions. However, further research focusing on aspects such as rheology, early age hydration, and pumping characteristics is needed before these cements can be implemented in large-scale 3D printing-related projects.

5. Sustainability assessment of the concrete for 3D printing

5.1. Quantification of embodied impacts of the material used for 3DCP

The quantification of environmental impact in terms of CO_2 emissions and energy consumption of different conventional cementitious binder systems (OPC+SCMs) and alternative binder systems (LC3, Geopolymer concrete (GPC) and CSA) for 3D printing of concrete is explained in this section. Life cycle assessment is used as a tool to calculate the environmental impacts of the concretes used for 3D printing, broadly following the methodology given in ISO 14040 [167] and 14044 [168]. Concretes considered here were made in Chennai used

for 3D printing at IIT Madras using a gantry-based 3D printer by Tvasta [169]. The fresh properties, i.e. extrudability and buildability, were taken as the performance criteria for selecting the mixes. The initial static yield stress is considered as the functional indicator for extrudability and buildability of the mixes.

For calculating the environmental impacts, the system boundary considered in the assessment is cradle (ground) to gate, considering all processes until the concrete production, as shown in Fig. 3. This involves the extraction of raw materials for OPC production, extraction and transportation of sand, electricity production and consumption in mixing plant. Additionally, for GGBS (SLG) production, transportation of slag from the steel plant, and electricity used in grinding of GBS to GGBS are considered. Instead of using LC3 as a binder directly in concrete production, LC2 (Limestone calcined clay) is used as a SCM. Actual production data for OPC and SLG have been collected from a cement plant at Nandyal, Andhra Pradesh, India, which is located at a distance of 400 km from Chennai [170]. Clay is assumed to be calcined at the same cement plant and blended with limestone to get LC2. The energy consumed for calcination of clay is assumed to be 2.6 MJ/kg and corresponding impacts are calculated considering ground to gate boundary for a calcination process [170,171]. Similarly, silica fume (SF) and fly ash (PFA) are assumed to be transported from a nearby port (50 km away) and a thermal power plant (50 km away), respectively. Cut off criteria are followed and impacts only due to transportation of PFA and SF are considered and not for their production. The impacts associated with production of alkaline solution for geopolymer concrete are taken from the ecoinvent database [172]. Alternatively, the impacts of the production of the alkaine solutions can be calculated using country specific databases, as done by several other researchers [173–175]. Superplasticizers, accelerators and fibres used in the mixes are considered to not influence the total impact due to the small volumes. The impacts associated (ground to gate) with each type of binder are provided in Table 3. The complete framework used in calculating the environmental impact can be found elsewhere [170,171].

The mixes containing Class F fly ash (PFA) (@ 20% of total binder content), ground granulated blast furnace slag (SLG) (@ 50% of total binder), and limestone-calcined clay (LC2, @ 30% of total binder) as SCMs, and having same initial static yield stress of 1.6 kPa (measured using the vane shear apparatus, as described in Rahul et al. [19]), are compared in Fig. 4. Later in Fig. 5, the printable conventional and alternative binder systems given in Table 4 with different yield stress are compared. In Fig. 4(b), the mix with fly ash (PFA-20) is seen to have the highest CO_2 emissions followed by the mix with LC2 (LC2-30). The performance of the SLG mix is better than the other two mixes in terms of both emissions and energy consumption. The environmental impact of slag as a SCM in the printable mix comes out to be lower than the other two mixes, mainly due to high replacement of OPC with slag (50%). It is important to understand that in the assessment provided here, the static yield stress is taken as the only performance criterion for the comparisons. However, the actual buildability in terms of the number of layers printed has not been specifically considered – this would be another important factor to adjudge the suitability of the different material types.

Fig. 5 shows the environmental impact of several printable mixes with conventional and alternative binder systems. The static shear yield stress and its measuring method for these mixes are given in Table 4. Since these mixes were used by different authors, printability is considered as the basis for comparison in Fig. 5. The binder contents also vary among the mixes; hence, the quantified numbers are normalized with total binder content ($kgCO_2$/kg of binder and MJ/kg of binder) as given in Table 4. Generally, ternary binder systems like PFA+SF and LC2, and GPC have lower CO_2 emissions. The PFA-40+SF-20 mix exhibits the least CO_2 emissions and energy consumed because of the higher OPC replacement level (60%). Since high molarity alkali solution was used in GPC-1 and GPC-2 mixes, energy consumed is higher compared to that of the GPC-2, GPC-3 and GPC-4 mixes. The energy consumed for the production of the alkali activator solution is higher and hence, the GPC mixes have higher energy consumption. The LC2-60 mix has lower environmental impact compared to LC2-30, showing that concretes can be sustainable at high dosages of LC2.

The carbon footprint per kg of the binder is the lowest for the GPC mixes followed by PFA-40+SF-20, SLG and LC2-60 mix. The energy consumed per kg of the binder is lowest in case of the ternary mixes (PFA 40% +SF 60%), and is similar for the SLG and GPC mixes. The ternary and GPC mixes contain large amounts of fly ash and SF, which are considered as waste materials in this study, contributing to the lower impact. However, many of the studies reported with GPC make use of processed fly ash and micro silica, which may have a higher impact. The results of the current study indicate that conventional binder systems with higher replacement level of SCMs can perform on par with alternative binder systems with respect to energy and emissions. The OPC-CSA mix with 7% CSA binder seems to perform similar to conventional mixes, and thus can be a promising alternative with higher replacement levels.

For the evolution of concrete 3D printing technology as a sustainable alternative for construction, all the relevant phases, including material production and mixing, transportation, pumping, printing, maintenance and recycling potential, should be analyzed. Subsequently, these phases can be optimized with respect to material utilization, carbon footprint and energy consumption, to yield the most sustainable options.

6. Summary

The broader aspects of 3DCP in terms of the factors that could influence the sustainability, along with the different processes and phases in the life cycle of a structure, have been discussed. The generic life cycle of 3DCP from cradle to cradle is shown, highlighting phases such as material production, transportation, construction (printing), operation and end-of-life (recycle and reuse). The material production stage, which is one of the phases responsible for a majority of the impact, has been assessed considering a range of printable concretes. CO_2 emissions and energy consumed are used as indicators to measure the sustainability potential of materials.

The literature pertaining to the influence of SCMs, aggregates and w/b ratio on the sustainability of printable conventional cementitious based mixes has been reviewed in the paper. To modify the mixes in terms of rheological parameters, different SCMs like fly ash, GGBS, and silica fume have been widely used. These SCMs tend to enhance the sustainability of 3D printable mixes by reducing the cement content. Further, most printable mixes only have fine aggregates, with a maximum size of 2 mm, which can lead to higher CO_2 emissions and energy consumed compared to conventional concrete due to the higher binder content. These aspects have been critically analyzed so that the advantages and limitations of unconventional components 3D printable concretes are highlighted in the context of sustainability. It is shown, through an illustrative the assessment of concretes with the same initial static yield stress, that ternary binders with high dosages of SCMs and geopolymer could be good alternatives, considering fly ash and slag to be available in large quantities.

Declaration of competing interest

The authors declare that they have no known competing financial interests or personal relationships that could have appeared to influence the work reported in this paper.

References

[1] G. Vantyghem, W. De Corte, E. Shakour, O. Amir, 3D printing of a post-tensioned concrete girder designed by topology optimization, Autom. ConStruct. 112 (2020) 103084, https://doi.org/10.1016/j.autcon.2020.103084.

[2] T.A.M. Salet, Z.Y. Ahmed, F.P. Bos, H.L.M. Laagland, Design of a 3D printed concrete bridge by testing, Virtual Phys. Prototyp. 13 (2018) 222–236, https://doi.org/10.1080/17452759.2018.1476064.

[3] J. Bekkering, B. Kuit, A. Biffi, Z.Y. Ahmed, Architectonic explorations of the possibilities of 3D concrete printing: the historic building fragment as inspiration for new applications with 3D concrete printing in architecture, in: F.P. Bos, S. S. Lucas, R.J.M. Wolfs, T.A.M. Salet (Eds.), Second RILEM Int. Conf. Concr. Digit. Fabr, Springer International Publishing, Cham, 2020, pp. 1078–1090.

[4] P. Martens, M. Mathot, F. Bos, J. Coenders, Optimising 3D printed concrete structures using topology optimisation, in: D.A. Hordijk, M. Luković (Eds.), High Tech Concr. Where Technol. Eng. Meet, Springer International Publishing, Cham, 2018, pp. 301–309.

[5] D. Asprone, F. Auricchio, C. Menna, V. Mercuri, 3D printing of reinforced concrete elements: technology and design approach, Construct. Build. Mater. 165 (2018) 218–231, https://doi.org/10.1016/j.conbuildmat.2018.01.018.

[6] I. Agustí-Juan, F. Müller, N. Hack, T. Wangler, G. Habert, Potential benefits of digital fabrication for complex structures: environmental assessment of a robotically fabricated concrete wall, J. Clean. Prod. 154 (2017) 330–340, https://doi.org/10.1016/j.jclepro.2017.04.002.

[7] J. Opon, M. Henry, An indicator framework for quantifying the sustainability of concrete materials from the perspectives of global sustainable development, J. Clean. Prod. 218 (2019) 718–737, https://doi.org/10.1016/j.jclepro.2019.01.220.

[8] I. Agustí-Juan, G. Habert, Environmental design guidelines for digital fabrication, J. Clean. Prod. 142 (2017) 2780–2791, https://doi.org/10.1016/j.jclepro.2016.10.190.

[9] G. De Schutter, K. Lesage, V. Mechtcherine, V.N. Nerella, G. Habert, A.J. Isolda, Vision of 3D printing with concrete—technical, economic and environmental potentials, Cement Concr. Res. 112 (2018) 25–36, https://doi.org/10.1016/j.cemconres.2018.06.001.

[10] A.V. Rahul, M. Santhanam, Evaluating the printability of concretes containing lightweight coarse aggregates, Cement Concr. Compos. 109 (2020) 103570, https://doi.org/10.1016/j.cemconcomp.2020.103570.

[11] G. Ma, Y. Li, L. Wang, J. Zhang, Z. Li, Real-time quantification of fresh and hardened mechanical property for 3D printing material by intellectualization with piezoelectric transducers, Construct. Build. Mater. 241 (2020) 117982, https://doi.org/10.1016/j.conbuildmat.2019.117982.

[12] X. Zhang, M. Li, J.H. Lim, Y. Weng, Y.W.D. Tay, H. Pham, Q.C. Pham, Large-scale 3D printing by a team of mobile robots, Autom. ConStruct. 95 (2018) 98–106, https://doi.org/10.1016/j.autcon.2018.08.004.

[13] Y. Weng, M. Li, Z. Liu, W. Lao, B. Lu, D. Zhang, M.J. Tan, Printability and fire performance of a developed 3D printable fibre reinforced cementitious composites under elevated temperatures, Virtual Phys. Prototyp. 14 (2019) 284–292, https://doi.org/10.1080/17452759.2018.1555046.

[14] B. Panda, M.J. Tan, Experimental study on mix proportion and fresh properties of fly ash based geopolymer for 3D concrete printing, Ceram. Int. 44 (2018) 10258–10265, https://doi.org/10.1016/j.ceramint.2018.03.031.

[15] V.N. Nerella, M. Krause, V. Mechtcherine, Direct printing test for buildability of 3D-printable concrete considering economic viability, Autom. ConStruct. 109 (2020) 102986, https://doi.org/10.1016/j.autcon.2019.102986.

[16] V.N. Nerella, M. Näther, A. Iqbal, M. Butler, V. Mechtcherine, Inline quantification of extrudability of cementitious materials for digital construction, Cement Concr. Compos. 95 (2019) 260–270, https://doi.org/10.1016/j.cemconcomp.2018.09.015.

[17] B. Lu, Y. Weng, M. Li, Y. Qian, K.F. Leong, M.J. Tan, S. Qian, A systematical review of 3D printable cementitious materials, Construct. Build. Mater. 207 (2019) 477–490, https://doi.org/10.1016/j.conbuildmat.2019.02.144.

[18] A.V. Rahul, M. Santhanam, H. Meena, Z. Ghani, 3D printable concrete: mixture design and test methods, Cement Concr. Compos. 97 (2019) 13–23, https://doi.org/10.1016/j.cemconcomp.2018.12.014.

[19] A.V. Rahul, A. Sharma, M. Santhanam, A desorptivity-based approach for the assessment of phase separation during extrusion of cementitious materials, Cement Concr. Compos. 108 (2020) 103546, https://doi.org/10.1016/j.cemconcomp.2020.103546.

[20] ACI 304.2R-96, Placing Concrete by Pumping Methods, 2008.

[21] Y. Vanhove, K.H. Khayat, Forced bleeding test to assess stability of flowable concrete, ACI Mater. J. 113 (2016) 753–758, https://doi.org/10.14359/51689240.

[22] N. Roussel, Rheological requirements for printable concretes, Cement Concr. Res. 112 (2018) 76–85, https://doi.org/10.1016/j.cemconres.2018.04.005.

[23] J.H. Kim, S.H. Kwon, S. Kawashima, H.J. Yim, Rheology of cement paste under high pressure, Cement Concr. Compos. 77 (2017) 60–67, https://doi.org/10.1016/j.cemconcomp.2016.11.007.

[24] N. Roussel, A thixotropy model for fresh fluid concretes: theory, validation and applications, Cement Concr. Res. 36 (2006) 1797–1806, https://doi.org/10.1016/j.cemconres.2006.05.025.

[25] A. Perrot, D. Rangeard, A. Pierre, Structural built-up of cement-based materials used for 3D-printing extrusion techniques, Mater. Struct. 49 (2016) 1213–1220, https://doi.org/10.1617/s11527-015-0571-0.

[26] J. Kruger, S. Zeranka, G. van Zijl, A rheology-based quasi-static shape retention model for digitally fabricated concrete, Construct. Build. Mater. 254 (2020) 119241, https://doi.org/10.1016/j.conbuildmat.2020.119241.

[27] H. Jeong, S.J. Han, S.H. Choi, Y.J. Lee, S.T. Yi, K.S. Kim, Rheological property criteria for buildable 3D printing concrete, Materials 12 (2019) 1–21, https://doi.org/10.3390/ma12040657.

[28] R.J.M. Wolfs, F.P. Bos, T.A.M. Salet, Early age mechanical behaviour of 3D printed concrete: numerical modelling and experimental testing, Cement Concr. Res. 106 (2018) 103–116, https://doi.org/10.1016/j.cemconres.2018.02.001.

[29] R.J.M. Wolfs, A.S.J. Suiker, Structural failure during extrusion-based 3D printing processes, Int. J. Adv. Manuf. Technol. 104 (2019) 565–584, https://doi.org/10.1007/s00170-019-03844-6.

[30] B. Panda, J.H. Lim, M.J. Tan, Mechanical properties and deformation behaviour of early age concrete in the context of digital construction, Compos. B Eng. 165 (2019) 563–571, https://doi.org/10.1016/j.compositesb.2019.02.040.

[31] B.N. Diggs-McGee, E.L. Kreiger, M.A. Kreiger, M.P. Case, Print time vs. elapsed time: a temporal analysis of a continuous printing operation for additive constructed concrete, Addit. Manuf. 28 (2019) 205–214, https://doi.org/10.1016/j.addma.2019.04.008.

[32] A.S.J. Suiker, Mechanical performance of wall structures in 3D printing processes: theory, design tools and experiments, Int. J. Mech. Sci. 137 (2018) 145–170, https://doi.org/10.1016/j.ijmecsci.2018.01.010.

[33] Y. Zhang, Y. Zhang, G. Liu, Y. Yang, M. Wu, B. Pang, Fresh properties of a novel 3D printing concrete ink, Construct. Build. Mater. 174 (2018) 263–271, https://doi.org/10.1016/j.conbuildmat.2018.04.115.

[34] T. Marchment, J. Sanjayan, M. Xia, Method of enhancing interlayer bond strength in construction scale 3D printing with mortar by effective bond area amplification, Mater. Des. 169 (2019) 107684, https://doi.org/10.1016/j.matdes.2019.107684.

[35] T. Marchment, M. Xia, E. Dodd, J. Sanjayan, B. Nematollahi, Effect of delay time on the mechanical properties of extrusion-based 3D printed concrete, in: ISARC 2017 - Proc. 34th Int. Symp. Autom. Robot. Constr., 2017, pp. 240–245, https://doi.org/10.22260/isarc2017/0032.

[36] E. Keita, H. Bessaies-Bey, W. Zuo, P. Belin, N. Roussel, Weak bond strength between successive layers in extrusion-based additive manufacturing: measurement and physical origin, Cement Concr. Res. 123 (2019), https://doi.org/10.1016/j.cemconres.2019.105787.

[37] V.N. Nerella, V. Mechtcherine, Studying the printability of fresh concrete for formwork-free concrete onsite 3D printing technology (CONPrint3D), in: J. G. Sanjayan, A. Nazari, B. Nematollahi (Eds.), 3D Concr. Print. Technol., Butterworth-Heinemann, 2019, pp. 333–347, https://doi.org/10.1016/B978-0-12-815481-6.00016-6.

[38] J. Kruger, S. Zeranka, G. van Zijl, 3D concrete printing: a lower bound analytical model for buildability performance quantification, Autom. ConStruct. 106 (2019) 102904, https://doi.org/10.1016/j.autcon.2019.102904.

[39] G. Ma, Z. Li, L. Wang, Printable properties of cementitious material containing copper tailings for extrusion based 3D printing, Construct. Build. Mater. 162 (2018) 613–627, https://doi.org/10.1016/j.conbuildmat.2017.12.051.

[40] Y. Chen, C.R. Rodriguez, Z. Li, B. Chen, O. Çopuroğlu, E. Schlangen, Effect of different grade levels of calcined clays on fresh and hardened properties of ternary-blended cementitious materials for 3D printing, Cement Concr. Compos. 114 (2020) 103708, https://doi.org/10.1016/j.cemconcomp.2020.103708.

[41] A. Kazemian, X. Yuan, E. Cochran, B. Khoshnevis, Cementitious materials for construction-scale 3D printing: laboratory testing of fresh printing mixture, Construct. Build. Mater. 145 (2017) 639–647, https://doi.org/10.1016/j.conbuildmat.2017.04.015.

[42] T.T. Le, S.A. Austin, S. Lim, R.A. Buswell, A.G. Gibb, T. Thorpe, Mix design and fresh properties for high-performance printing concrete, Mater. Struct. 45 (8) (2012) 1221–1232.

[43] C. Gosselin, R. Duballet, P. Roux, N. Gaudillière, J. Dirrenberger, P. Morel, Large-scale 3D printing of ultra-high performance concrete—a new processing route for architects and builders, Mater. Des. 100 (2016) 102–109.

[44] B. Panda, S. Ruan, C. Unluer, M. Jen, Improving the 3D printability of high volume fly ash mixtures via the use of nano attapulgite clay, Compos. Part B 165 (2019) 75–83, https://doi.org/10.1016/j.compositesb.2018.11.109.

[45] J. Van Der Putten, M. De Volder, P. Van den Heede, G. De Schutter, K. Van Tittelboom, 3D printing of concrete: the influence on chloride penetration, in: F. P. Bos, S.S. Lucas, R.J.M. Wolfs, T.A.M. Salet (Eds.), Second RILEM Int. Conf. Concr. Digit. Fabr. – Digit. Concr, Springer, 2020, pp. 500–507, https://doi.org/10.1007/978-3-030-49916-7_51.

[46] J. Van Der Putten, M. Azima, P. Van den Heede, T. Van Mullem, D. Snoeck, C. Carminati, J. Hovind, P. Trtik, G. De Schutter, K. Van Tittelboom, Neutron radiography to study the water ingress via the interlayer of 3D printed cementitious materials for continuous layering, Construct. Build. Mater. 258 (2020) 119587, https://doi.org/10.1016/j.conbuildmat.2020.119587.

[47] C. Schröfl, V.N. Nerella, V. Mechtcherine, Capillary water intake by 3D-printed concrete visualised and quantified by neutron radiography, in: T. Wangler, R. J. Flatt (Eds.), 1st RILEM Inter. Conf. On Conc. and Digi. Fabri. – Digi. Conc. 2018, Springer, 2019, pp. 217–224, https://doi.org/10.1007/978-3-319-99519-9_20.

[48] D. Weger, D. Lowke, C. Gehlen, D. Talke, K. Henke, Additive manufacturing of concrete elements using selective cement paste intrusion–effect of layer orientation on strength and durability, in: T. Wangler, R.J. Flatt (Eds.), 1st RILEM Inter. Conf. On Conc. and Digi. Fabri. – Digi. Conc. 2018, Springer, 2019, pp. 2016–2017.u.

[49] J.J. Assaad, F. Hamzeh, B. Hamad, Qualitative assessment of interfacial bonding in 3D printing concrete exposed to frost attack, case study, Constr. Mater. 13 (2020), e00357, https://doi.org/10.1016/j.cscm.2020.e00357.

[50] W.J. Long, Y. Gu, J. Liao, F. Xing, Sustainable design and ecological evaluation of low binder self-compacting concrete, J. Clean. Prod. 167 (2017) 317–325, https://doi.org/10.1016/j.jclepro.2017.08.192.

[51] H. Yazici, The effect of silica fume and high-volume Class C fly ash on mechanical properties, chloride penetration and freeze-thaw resistance of self-compacting

concrete, Construct. Build. Mater. 22 (2008) 456–462, https://doi.org/10.1016/j.conbuildmat.2007.01.002.

[52] W. Meng, A. Kumar, K.H. Khayat, Effect of silica fume and slump-retaining polycarboxylate-based dispersant on the development of properties of portland cement paste, Cement Concr. Compos. 99 (2019) 181–190, https://doi.org/10.1016/j.cemconcomp.2019.03.021.

[53] H. Vikan, H. Justnes, Rheology of cementitious paste with silica fume or limestone, Cement Concr. Res. 37 (2007) 1512–1517, https://doi.org/10.1016/j.cemconres.2007.08.012.

[54] M.C.G. Juenger, R. Siddique, Recent advances in understanding the role of supplementary cementitious materials in concrete, Cement Concr. Res. 78 (2015) 71–80, https://doi.org/10.1016/j.cemconres.2015.03.018.

[55] K.H. Khayat, A. Yahia, M. Sayed, Effect of supplementary cementitious materials on rheological properties, bleeding, and strength of structural grout, ACI Mater. J. 105 (2008) 585–593, https://doi.org/10.14359/20200.

[56] M. Cyr, Influence of supplementary cementitious materials (SCMs) on concrete durability, in: F. Pacheco –Torgal, S. Jalai, J. Labrincha, V.M. John (Eds.), Eco-Efficient Concrete, Woodhead Publishing, 2013, pp. 153–197, https://doi.org/10.1533/9780857098993.2.153.

[57] M.A.M. Johari, J.J. Brooks, S. Kabir, P. Rivard, Influence of supplementary cementitious materials on engineering properties of high strength concrete, Construct. Build. Mater. 25 (2011) 2639–2648, https://doi.org/10.1016/j.conbuildmat.2010.12.013.

[58] Y. Weng, B. Lu, M.J. Tan, S. Qian, Rheology and printability of engineered cementitious composites—a literature review, in: Proc. Of the 2nd Inter. Conf. on Prog. in Add. Manuf, Research Publishing, Singapore, 2016, pp. 427–432.

[59] B. Panda, M.J. Tan, Material properties of 3D printable high-volume slag cement, in: Proc. Of the First Inter. Conf. on 3D Const. Prin. (3DcP) in Conjunction with the 6th Inter. Conf. on Innov. Prod. and Const. (IPC 2018), 2018. Melbourne, Australia, Appl. Sci.

[60] D.P. Bentz, S.Z. Jones, I.R. Bentz, M.A. Peltz, Towards the formulation of robust and sustainable cementitious binders for 3-D additive construction by extrusion, Construct. Build. Mater. 175 (2018) 215–224, https://doi.org/10.1016/j.conbuildmat.2018.04.167.

[61] K. Scrivener, F. Martirena, S. Bishnoi, S. Maity, Calcined clay limestone cements (LC3), Cement Concr. Res. 114 (2018) 49–56, https://doi.org/10.1016/j.cemconres.2017.08.017.

[62] T. Matschei, B. Lothenbach, F.P. Glasser, The role of calcium carbonate in cement hydration, Cement Concr. Res. 37 (2007) 551–558, https://doi.org/10.1016/j.cemconres.2006.10.013.

[63] M. Glavind, Sustainability of Cement, Concrete and Cement Replacement Materials in Construction, Woodhead Publishing Limited, Cambridge, UK, 2009.

[64] R. Snellings, Assessing, understanding and unlocking supplementary cementitious materials, RILEM Tech. Lett. 1 (2016) 50–55.

[65] Y. Chen, F. Veer, O. Copuroglu, E. Schlangen, Feasibility of using low CO$_2$ concrete alternatives in extrusion-based 3D concrete printing. Proc. Of the RILEM Inter. Conf. on Conc. and Digi, . Fabri. Zurich, Switzerland, 2018, pp. 269–276.

[66] M.A.B. Beigh, V.N. Nerella, C. Schröfl, V. Mechtcherine, Studying the rheological behavior of limestone calcined clay cement (LC3) mixtures in the context of extrusion- based 3D-printing, in: Shashank Bishnoi (Ed.), Calcined Clays for Sustainable Concrete, Proceedings of 3rd Int. Conf. Calcined Clays Sustain. Concr, . Springer, 2020, pp. 229–236.

[67] P.-C. Aïtcin, in: P.C. Hewlett, M.B.T.-L.C. of C, C, (Fifth E. Liska (Eds.), The Influence of the Water/cement Ratio on the Sustainability of Concrete, Butterworth-Heinemann, 2019, pp. 807–826, https://doi.org/10.1016/B978-0-08-100773-0.00017-4.

[68] V. Mechtcherine, V.N. Nerella, F. Will, M. Näther, J. Otto, M. Krause, Large-scale digital concrete construction – CONPrint3D concept for on-site, monolithic 3D-printing, Autom. ConStruct. 107 (2019) 102933, https://doi.org/10.1016/j.autcon.2019.102933.

[69] N. Roussel, J. Spangenberg, J. Wallevik, R. Wolfs, Numerical simulations of concrete processing: from standard formative casting to additive manufacturing, Cement Concr. Res. 135 (2020) 106075, https://doi.org/10.1016/j.cemconres.2020.106075.

[70] V.C. Li, F.P. Bos, K. Yu, W. McGee, T.Y. Ng, S.C. Figueiredo, K. Nefs, V. Mechtcherine, V.N. Nerella, J. Pan, G.P.A.G. van Zijl, P.J. Kruger, On the emergence of 3D printable engineered, strain hardening cementitious composites (ECC/SHCC), Cement Concr. Res. 132 (2020) 106038.

[71] G. Ma, N.M. Salman, L. Wang, F. Wang, A novel additive mortar leveraging internal curing for enhancing interlayer bonding of cementitious composite for 3D printing, Construct. Build. Mater. 244 (2020) 118305, https://doi.org/10.1016/j.conbuildmat.2020.118305.

[72] C. Menna, J. Mata-Falcón, F.P. Bos, G. Vantyghem, L. Ferrara, D. Asprone, T. Salet, W. Kaufmann, Opportunities and challenges for structural engineering of digitally fabricated concrete, Cement Concr. Res. 133 (2020) 106079, https://doi.org/10.1016/j.cemconres.2020.106079.

[73] W. Shen, R. Dong, J. Li, M. Zhou, W. Ma, J. Zha, Experimental investigation on aggregate interlocking concrete prepared with scattering–filling coarse aggregate process, Construct. Build. Mater. 24 (11) (2010) 2312–2316, https://doi.org/10.1016/j.conbuildmat.2010.04.023.

[74] M.T. Souza, I.M. Ferreira, E. Guzi de Moraes, L. Senff, A.P. Novaes de Oliveira, 3D printed concrete for large-scale buildings: an overview of rheology, printing parameters, chemical admixtures, reinforcements, and economic and environmental prospects, J. Build. Eng. 32 (2020) 101833, https://doi.org/10.1016/j.jobe.2020.101833.

[75] F. Storch, K. Krenzer, V.N. Nerella, M. Simon, F. Will, V. Mechtcherine, Development of a printhead for large-scale, extrusion-based additive manufacturing with coarse aggregate concrete, Construct. Print. Technol. 4 (2020) 16–21.

[76] I. Ivanova, V. Mechtcherine, Effects of volume fraction and surface area of aggregates on the static yield stress and structural build- up of fresh concrete, 13, 2020, p. 1551, https://doi.org/10.3390/ma13071551, 7.

[77] S. Yu, H. Du, J. Sanjayan, Aggregate-bed 3D concrete printing with cement paste binder, Cement Concr. Res. 136 (2020) 106169, https://doi.org/10.1016/j.cemconres.2020.106169.

[78] E.R. Teixeira, R. Mateus, A.F. Camões, L. Bragança, F.G. Branco, Comparative environmental life-cycle analysis of concretes using biomass and coal fly ashes as partial cement replacement material, J. Clean. Prod. 112 (2016) 2221–2230, https://doi.org/10.1016/j.jclepro.2015.09.124.

[79] S.A.A.M. Fennis, J.C. Walraven, Using particle packing technology for sustainable concrete mixture design, Heron 57 (2011) 73–102.

[80] A. Kwan, C. Mora, Effects of various, shape parameters on packing of aggregate particles, Mag. Concr. Res. 53 (2002) 91–100.

[81] E. Rozière, S. Granger, P. Turcry, A. Loukili, Influence of paste volume on shrinkage cracking and fracture properties of self-compacting concrete, Cement Concr. Compos. 29 (2007) 626–636, https://doi.org/10.1016/j.cemconcomp.2007.03.010.

[82] P. Goltermann, V. Johansen, L. Palbøl, Packing of aggregate: an alternative tool to determine the optimal aggregate mix, ACI Mater. J. 94 (1997) 435–443.

[83] A.K.H. Kwan, L.G. Li, Combined effects of water film thickness and paste film thickness on rheology of mortar, Mater. Struct. 45 (2012) 1359–1374, https://doi.org/10.1617/s11527-012-9837-y.

[84] H.S. Müller, R. Breiner, J.S. Moffatt, M. Haist, Design and properties of sustainable concrete, Procedia Eng. 95 (2014) 290–304, https://doi.org/10.1016/j.proeng.2014.12.189.

[85] G.H.A. Ting, Y.W.D. Tay, Y. Qian, M.J. Tan, Utilization of recycled glass for 3D concrete printing: rheological and mechanical properties, J. Mater. Cycles Waste Manag. 21 (2019) 994–1003, https://doi.org/10.1007/s10163-019-00857-x.

[86] Y. Han, Z. Yang, T. Ding, J. Xiao, Environmental and economic assessment on 3D printed buildings with recycled concrete, J. Clean. Prod. 278 (2021) 123884, https://doi.org/10.1016/j.jclepro.2020.123884.

[87] S. Pradhan, B.R. Tiwari, S. Kumar, S.V. Barai, Comparative LCA of recycled and natural aggregate concrete using particle packing method and conventional method of design mix, J. Clean. Prod. 228 (2019) 679–691, https://doi.org/10.1016/j.jclepro.2019.04.328.

[88] L.G. Li, A.K.H. Kwan, Concrete mix design based on water film thickness and paste film thickness, Cement Concr. Compos. 39 (2013) 33–42, https://doi.org/10.1016/j.cemconcomp.2013.03.021.

[89] D.P. Bentz, E.J. Garboczi, C.J. Haecker, O.M. Jensen, Effects of cement particle size distribution on performance properties of Portland cement-based materials, Cement Concr. Res. 29 (1999) 1663–1671, https://doi.org/10.1016/S0008-8846(99)00163-5.

[90] I.B. Celik, The effects of particle size distribution and surface area upon cement strength development, Powder Technol. 188 (2009) 272–276, https://doi.org/10.1016/j.powtec.2008.05.007.

[91] T.S. Zhang, Q.J. Yu, J.X. Wei, P.P. Zhang, Effects of size fraction on composition and fundamental properties of Portland cement, Construct. Build. Mater. 25 (2011) 3038–3043, https://doi.org/10.1016/j.conbuildmat.2011.01.005.

[92] T. Knudsen, The dispersion model for hydration of Portland cement I. General concepts, Cement Concr. Compos. 14 (1984) 622–630, https://doi.org/10.1016/0008-8846(84)90024-3.

[93] D.P. Bentz, Replacement of "coarse" cement particles by inert fillers in low w/c ratio concretes: II. Experimental validation, Cement Concr. Compos. 35 (2005) 185–188, https://doi.org/10.1016/j.cemconres.2004.09.003.

[94] B. Panda, G.V.P. B Singh, C. Unluer, M.J. Tan, Synthesis and characterization of one-part geopolymers for extrusion based 3D concrete printing, J. Clean. Prod. 220 (2019) 610–619, https://doi.org/10.1016/j.jclepro.2019.02.185.

[95] H. Alghamdi, S.A.O. Nair, N. Neithalath, Insights into material design, extrusion rheology, and properties of 3D-printable alkali-activated fly ash-based binders, Mater. Des. 167 (2019) 107634, https://doi.org/10.1016/j.matdes.2019.107634.

[96] B. Panda, C. Unluer, M.J. Tan, Extrusion and rheology characterization of geopolymer nanocomposites used in 3D printing, Compos. B Eng. 176 (2019) 107290, https://doi.org/10.1016/j.compositesb.2019.107290.

[97] S.H. Bong, B. Nematollahi, A. Nazari, M. Xia, J. Sanjayan, Method of optimisation for ambient temperature cured sustainable geopolymers for 3D printing construction applications, Materials 12 (2019) PMC6470972, https://doi.org/10.3390/ma12060902.

[98] S.H. Bong, B. Behzad, N. Ali, X. Ming, S.G. Jay, Fresh and hardened properties of 3D printable Geopolymer cured in ambient temperature, in: T. wangler, R.J. Flatt (Eds.), 1st RILEM Inter. Conf. On Conc. and Digi. Fabri. – Digi. Conc. 2018, Springer, 2018, pp. 3–11.

[99] B. Nematollahi, M. Xia, S.H. Bong, S. Jay, W. Timothy, F.J. Robert, Hardened properties of 3D printable 'one-part' geopolymer for construction applications, in: T. wangler, R.J. Flatt (Eds.), 1st RILEM Inter. Conf. On Conc. and Digi. Fabri. – Digi. Conc. 2018, Springer, 2019, pp. 190–199.

[100] B. Panda, C. Unluer, M.J. Tan, Investigation of the rheology and strength of geopolymer mixtures for extrusion-based 3D printing, Cement Concr. Compos. 94 (2018) 307–314, https://doi.org/10.1016/j.cemconcomp.2018.10.002.

[101] S. Muthukrishnan, S. Ramakrishnan, J. Sanjayan, Effect of microwave heating on interlayer bonding and buildability of geopolymer 3D concrete printing,

Construct. Build. Mater. 265 (2020) 120786, https://doi.org/10.1016/j.conbuildmat.2020.120786.

[102] B. Panda, S. Ruan, C. Unluer, M.J. Tan, Investigation of the properties of alkali-activated slag mixes involving the use of nanoclay and nucleation seeds for 3D printing, Compos. B Eng. 186 (2020) 107826, https://doi.org/10.1016/j.compositesb.2020.107826.

[103] C. Sun, J. Xiang, M. Xu, Y. He, Z. Tong, X. Cui, 3D extrusion free forming of geopolymer composites: materials modification and processing optimization, J. Clean. Prod. 258 (2020) 120986, https://doi.org/10.1016/j.jclepro.2020.120986.

[104] B. Nematollahi, P. Vijay, J. Sanjayan, A. Nazari, M. Xia, V.N. Nerella, V. Mechtcherine, Effect of polypropylene fibre addition on properties of geopolymers made by 3D printing for digital construction, Materials 11 (2018) 2352, https://doi.org/10.3390/ma11122352.

[105] S. Al-Qutaifi, A. Nazari, A. Bagheri, Mechanical properties of layered geopolymer structures applicable in concrete 3D-printing, Construct. Build. Mater. 176 (2018) 690–699, https://doi.org/10.1016/j.conbuildmat.2018.04.195.

[106] M.C.G. Juenger, R. Snellings, S.A. Bernal, Supplementary cementitious materials: new sources, characterization, and performance insights, Cement Concr. Res. 122 (2019) 257–273, https://doi.org/10.1016/j.cemconres.2019.05.008.

[107] D. Jiao, C. Shi, Q. Yuan, X. An, Y. Liu, H. Li, Effect of constituents on rheological properties of fresh concrete-A review, Cement Concr. Compos. 83 (2017) 146–159, https://doi.org/10.1016/j.cemconcomp.2017.07.016.

[108] K. Vance, A. Kumar, G. Sant, N. Neithalath, The rheological properties of ternary binders containing Portland cement, limestone, and metakaolin or fly ash, Cement Concr. Res. 52 (2013) 196–207, https://doi.org/10.1016/j.cemconres.2013.07.007.

[109] K. Ma, G. Long, Y. Xie, R. Zhu, Rheological properties of compound pastes with cement-fly ash-limestone powder, J. Chin. Ceram. Soc. 41 (2013) 582–587, https://doi.org/10.7521/j.issn.0454-5648.2013.05.02.

[110] E. Berodier, K. Scrivener, Understanding the filler effect on the nucleation and growth of C-S-H, J. Am. Ceram. Soc. 97 (2014) 3764–3773, https://doi.org/10.1111/jace.13177.

[111] K.L. Scrivener, Options for the future of cement, Indian Concr. J. 88 (2014) 11–21.

[112] M. Antoni, J. Rossen, F. Martirena, K. Scrivener, Cement substitution by a combination of metakaolin and limestone, Cement Concr. Res. 42 (2012) 1579–1589, https://doi.org/10.1016/j.cemconres.2012.09.006.

[113] W. Huang, H. Kazemi-Kamyab, W. Sun, K. Scrivener, Effect of replacement of silica fume with calcined clay on the hydration and microstructural development of eco-UHPFRC, Mater. Des. 121 (2017) 36–46, https://doi.org/10.1016/j.matdes.2017.02.052.

[114] L.M. Vizcaíno-Andrés, S. Sánchez-Berriel, S. Damas-Carrera, A. Pérez-Hernández, K.L. Scrivener, J.F. Martirena-Hernández, Industrial trial to produce a low clinker, low carbon cement, Mater. Construcción 65 (2015) e045, https://doi.org/10.3989/mc.2015.00614.

[115] A.C. Emmanuel, P. Haldar, S. Maity, S. Bishnoi, Second pilot production of limestone calcined clay cement in India: the experience, Indian Concr. J. 90 (2016) 57–63.

[116] F. Avet, R. Snellings, A. Alujas Diaz, M. Ben Haha, K. Scrivener, Development of a new rapid, relevant and reliable (R3) test method to evaluate the pozzolanic reactivity of calcined kaolinitic clays, Cement Concr. Res. 85 (2016) 1–11, https://doi.org/10.1016/j.cemconres.2016.02.015.

[117] A. Alujas, R. Fernández, R. Quintana, K.L. Scrivener, F. Martirena, Pozzolanic reactivity of low grade kaolinitic clays: influence of calcination temperature and impact of calcination products on OPC hydration, Appl. Clay Sci. 108 (2015) 94–101, https://doi.org/10.1016/j.clay.2015.01.028.

[118] J. Skibsted, R. Snellings, Reactivity of supplementary cementitious materials (SCMs) in cement blends, Cement Concr. Res. 124 (2019), https://doi.org/10.1016/j.cemconres.2019.105799.

[119] C. Shi, B. Qu, J.L. Provis, Recent progress in low-carbon binders, Cement Concr. Res. 122 (2019) 227–250, https://doi.org/10.1016/j.cemconres.2019.05.009.

[120] H. Maraghechi, F. Avet, H. Wong, H. Kamyab, K. Scrivener, Performance of Limestone Calcined Clay Cement (LC3) with various kaolinite contents with respect to chloride transport, Mater. Struct. 51 (2018) 1–17, https://doi.org/10.1617/s11527-018-1255-3.

[121] Z. Shi, M.R. Geiker, K. De Weerdt, T.A. Østnor, B. Lothenbach, F. Winnefeld, J. Skibsted, Role of calcium on chloride binding in hydrated Portland cement–metakaolin–limestone blends, Cement Concr. Res. 95 (2017) 205–216, https://doi.org/10.1016/j.cemconres.2017.02.003.

[122] Y. Dhandapani, M. Santhanam, Investigation on the microstructure-related characteristics to elucidate performance of composite cement with limestone-calcined clay combination, Cement Concr. Res. 129 (2020) 105959, https://doi.org/10.1016/j.cemconres.2019.105959.

[123] F. Avet, Investigation of the grade of calcined clays used as clinker substitute in limestone calcined clay cement (LC3) 8143, Ecole Polytechnique Federale de Lausanne -EPFl, Switzerland, 2017, p. 169. Ph.D. Thesis.

[124] Q.D. Nguyen, T. Kim, A. Castel, Mitigation of alkali-silica reaction by limestone calcined clay cement (LC3), Cement Concr. Res. 137 (2020) 106176, https://doi.org/10.1016/j.cemconres.2020.106176.

[125] R. Sposito, N. Beuntner, K.C. Thienel, Characteristics of calcined clay particles and their influence on the efficiency of superplasticizers, Cement Concr. Compos. 110 (2020) 103594, https://doi.org/10.1016/j.cemconcomp.2020.103594.

[126] H. Paiva, A. Velosa, P. Cachim, V.M. Ferreira, Effect of metakaolin dispersion on the fresh and hardened state properties of concrete, Cement Concr. Res. 42 (2012) 607–612, https://doi.org/10.1016/j.cemconres.2012.01.005.

[127] C. Perlot, P. Rougeau, S. Dehaudt, Slurry of metakaolin combined with limestone addition for self-compacted concrete - application for precast industry, Cement Concr. Compos. 44 (2013) 50–57, https://doi.org/10.1016/j.cemconcomp.2013.07.003.

[128] N. Nair, K. Mohammed Haneefa, M. Santhanam, R. Gettu, A study on fresh properties of limestone calcined clay blended cementitious systems, Construct. Build. Mater. 254 (2020) 119326, https://doi.org/10.1016/j.conbuildmat.2020.119326.

[129] F. Cassagnabère, P. Diederich, M. Mouret, G. Escadeillas, M. Lachemi, Impact of metakaolin characteristics on the rheological properties of mortar in the fresh state, Cement Concr. Compos. 37 (2013) 95–107, https://doi.org/10.1016/j.cemconcomp.2012.12.001.

[130] T.R. Muzenda, P. Hou, S. Kawashima, T. Sui, X. Cheng, The role of limestone and calcined clay on the rheological properties of LC3, Cement Concr. Compos. 107 (2020) 103516, https://doi.org/10.1016/j.cemconcomp.2020.103516.

[131] M.A.B. Beigh, V.N. Nerella, E. Secrieru, V. Mechtcherine, Structural Build-Up Behavior of Limestone Calcined Clay Cement (LC3) Pastes in the Context of Digital Concrete Construction, Conference Proceedings of 2nd International Conference on Rheology and Processing of Construction Materials (RhoCon2), 2019.

[132] Y. Chen, Z. Li, S. Chaves Figueiredo, O. Çopuroğlu, F. Veer, E. Schlangen, Limestone and Calcined Clay-based sustainable cementitious materials for 3D concrete printing: a fundamental study of extrudability and interlayer strength development, Appl. Sci. 9 (2019) 1809, https://doi.org/10.3390/app9091809.

[133] C. Aramburo, C. Pedrajas, V. Rahhal, M. González, R. Talero, Calcined clays for low carbon cement: rheological behaviour in fresh Portland cement pastes, Mater. Lett. 239 (2019) 24–28, https://doi.org/10.1016/j.matlet.2018.12.050.

[134] L. Lei, J. Plank, A study on the impact of different clay minerals on the dispersing force of conventional and modified vinyl ether based polycarboxylate superplasticizers, Cement Concr. Res. 60 (2014) 1–10, https://doi.org/10.1016/j.cemconres.2014.02.009.

[135] D. Marchon, S. Mantellato, A.B. Eberhardt, R.J. Flatt, Adsorption of chemical admixtures, in: P.- C Aitcin, R.J. Flatt (Eds.), Science and Technology of Concrete Admixtures, Woodhead Publishing, Elsevier Ltd, 2015, pp. 219–256, https://doi.org/10.1016/B978-0-08-100693-1.00010-2.

[136] E. Gartner, Industrially interesting approaches to "low-CO2" cements, Cement Concr. Res. 34 (2004) 1489–1498, https://doi.org/10.1016/j.cemconres.2004.01.021.

[137] J.H. Sharp, C.D. Lawrence, R. Yang, Calcium sulfoaluminate cements - low-energy cements, special cements or what? Adv. Cement Res. 11 (1999) 3–13, https://doi.org/10.1680/adcr.1999.11.1.3.

[138] M. Aranda, A.D. la Torre, Eco-efficient concrete: 18. Sulfoaluminate cement, Elseiver Inc., 2013. https://books.google.com/books?.hl=en&lr=&id=Wwt0DAAAQBAJ&oi=fnd&pg=PT4&dq=Calcium+sulphoaluminate+cements+–+Lowenergy+cements,+special+cements+or+what%3F',&ots=9PRR4JGKZA&sig=Zip-UfT0VUIIxSLO2N0UD4nceho. accessed August 15, 2020.

[139] J.W. Phair, Green chemistry for sustainable cement production and use, Green Chem. 8 (9) (2006) 763–780. https://doi.org/10.1039/b603997a.

[140] S.W. Tang, H.G. Zhu, Z.J. Li, E. Chen, H.Y. Shao, Hydration stage identification and phase transformation of calcium sulfoaluminate cement at early age, Construct. Build. Mater. 75 (2015) 11–18, https://doi.org/10.1016/j.conbuildmat.2014.11.006.

[141] Y. Liao, X. Wei, G. Li, Early hydration of calcium sulfoaluminate cement through electrical resistivity measurement and microstructure investigations, Construct. Build. Mater. 25 (2011) 1572–1579, https://doi.org/10.1016/j.conbuildmat.2010.09.042.

[142] N. Khalil, G. Aouad, K. El Cheikh, S. Rémond, Use of calcium sulfoaluminate cements for setting control of 3D-printing mortars, Construct. Build. Mater. 157 (2017) 382–391, https://doi.org/10.1016/j.conbuildmat.2017.09.109.

[143] S. Kim, T. Kim, B. Kim, H. dae Kim, J. Kim, H. Lee, Early hydration and hardening of OPC-CSA blends for cementitious structure of 3D printing, Adv. Appl. Ceram. 119 (7) (2020) 393–397, https://doi.org/10.1080/17436753.2020.1777505.

[144] M.K. Mohan, A.V. Rahul, G. De Schutter, K. Van Tittelboom, Early age hydration, rheology and pumping characteristics of CSA cement-based 3D printable concrete, Construct. Build. Mater. 275 (2021) 122136, https://doi.org/10.1016/J.CONBUILDMAT.2020.122136.

[145] M. Chen, X. Guo, Y. Zheng, L. Li, Z. Yan, P. Zhao, L. Lu, X. Cheng, Effect of tartaric acid on the printable, rheological and mechanical properties of 3D printing sulphoaluminate cement paste, Materials 11 (2018) 2417, https://doi.org/10.3390/ma11122417.

[146] M.K. Mohan, A.V. Rahul, K. Van Tittelboom, G. De Schutter, Extrusion-based concrete 3D printing from a material perspective: a state-of-the-art review, Cement Concr. Compos. (2020) 103855.

[147] J. Péra, J. Ambroise, New applications of calcium sulfoaluminate cement, Cement Concr. Res. 34 (2004) 671–676, https://doi.org/10.1016/j.cemconres.2003.10.019.

[148] P. Chaunsali, P. Mondal, Influence of calcium sulfoaluminate (CSA) cement content on expansion and hydration behavior of various ordinary portland cement-CSA blends, J. Am. Ceram. Soc. 98 (2015) 2617–2624, https://doi.org/10.1111/jace.13645.

[149] J. Bizzozero, C. Gosselin, K.L. Scrivener, Expansion mechanisms in calcium aluminate and sulfoaluminate systems with calcium sulfate, Cement Concr. Res. 56 (2014) 190–202, https://doi.org/10.1016/j.cemconres.2013.11.011.

[150] G. Ke, J. Zhang, S. Xie, T. Pei, Rheological behavior of calcium sulfoaluminate cement paste with supplementary cementitious materials, Construct. Build.

Mater. 243 (2020) 118234, https://doi.org/10.1016/j.conbuildmat.2020.118234.

[151] M. Chen, L. Yang, Y. Zheng, Y. Huang, L. Li, P. Zhao, S. Wang, L. Lu, X. Cheng, Yield stress and thixotropy control of 3D-printed calcium sulfoaluminate cement composites with metakaolin related to structural build-up, Construct. Build. Mater. 252 (2020) 119090, https://doi.org/10.1016/j.conbuildmat.2020.119090.

[152] M.K. Mohan, A.V. Rahul, K. Van Tittelboom, G. De Schutter, Rheological and pumping behaviour of 3D printable cementitious materials with varying aggregate content, Cement Concr. Res. 139 (2021) 106258, https://doi.org/10.1016/j.cemconres.2020.106258.

[153] K. Quillin, Performance of belite-sulfoaluminate cements, Cement Concr. Res. 31 (2001) 1341–1349, https://doi.org/10.1016/S0008-8846(01)00543-9.

[154] I. Janotka, L. Krajči, S.C. Mojumdar, Performance of sulphoaluminate-belite cement with high C4A 3S¯ content | Request PDF, Ceram. Silikaty. 51 (2007) 74–81.

[155] A.S. Bhatti, D. Dollimore, A. Dyer, Magnesia from seawater: a review, Clay Miner. 19 (1984) 865–875, https://doi.org/10.1180/claymin.1984.019.5.14.

[156] M. Shand, The Chemistry and Technology of Magnesia, John Wiley & Sons, 2006.

[157] N.T. Dung, C. Unluer, Carbonated MgO concrete with improved performance: the influence of temperature and hydration agent on hydration, carbonation and strength gain, Cement Concr. Compos. 82 (2017) 152–164, https://doi.org/10.1016/j.cemconcomp.2017.06.006.

[158] N.T. Dung, C. Unluer, Sequestration of CO2 in reactive MgO cement-based mixes with enhanced hydration mechanisms, Construct. Build. Mater. 143 (2017) 71–82, https://doi.org/10.1016/j.conbuildmat.2017.03.038.

[159] L. Mo, D.K. Panesar, Accelerated carbonation - a potential approach to sequester CO2 in cement paste containing slag and reactive MgO, Cement Concr. Compos. 43 (2013) 69–77, https://doi.org/10.1016/j.cemconcomp.2013.07.001.

[160] L.J. Vandeperre, A. Al-Tabbaa, Accelerated carbonation of reactive MgO cements, Adv. Cement Res. 19 (2007) 67–79, https://doi.org/10.1680/adcr.2007.19.2.67.

[161] C. Sonat, C.H. Lim, M. Liska, C. Unluer, Recycling and reuse of reactive MgO cements – a feasibility study, Construct. Build. Mater. 157 (2017) 172–181, https://doi.org/10.1016/j.conbuildmat.2017.09.068.

[162] A. Khalil, X. Wang, K. Celik, 3D printable magnesium oxide concrete: towards sustainable modern architecture, Addit. Manuf. 33 (2020) 101145, https://doi.org/10.1016/j.addma.2020.101145.

[163] S. Ruan, C. Unluer, Influence of mix design on the carbonation, mechanical properties and microstructure of reactive MgO cement-based concrete, Cement Concr. Compos. 80 (2017) 104–114, https://doi.org/10.1016/j.cemconcomp.2017.03.004.

[164] L.J. Vandeperre, M. Liska, A. Al-Tabbaa, Microstructures of reactive magnesia cement blends, Cement Concr. Compos. 30 (2008) 706–714, https://doi.org/10.1016/j.cemconcomp.2008.05.002.

[165] A.S. Wagh, Chemically Bonded Phosphate Ceramics: Twenty-First Century Materials with Diverse Applications, second ed., Elsevier, 2016 https://doi.org/10.1016/C2014-0-02562-2.

[166] Y. Weng, S. Ruan, M. Li, L. Mo, C. Unluer, M.J. Tan, S. Qian, Feasibility study on sustainable magnesium potassium phosphate cement paste for 3D printing, Construct. Build. Mater. 221 (2019) 595–603, https://doi.org/10.1016/j.conbuildmat.2019.05.053.

[167] ISO 14040, Environmental Management - Life Cycle Assessment - Principles and Framework, International Organization for Standardization, Geneva, 2006, p. 20.

[168] ISO 14044, Environmental Management – Life Cycle Assessment – Requirements and Guidelines, International Organization for Standardization, Geneva, 2006, p. 46.

[169] S. Bhattacherjee, A.V. Rahul, M. Santhanam, Concrete 3D printing – progress worldwide and in India, Indian Concr. J. 94 (9) (2020) 8–25.

[170] R. Gettu, R.G. Pillai, M. Santhanam, A.S. Basavaraj, S. Rathnarajan, B.S. Dhanya, Sustainability-based decision support framework for choosing concrete mixture proportions, Mater. Struct. 51 (2018) 1–16, https://doi.org/10.1617/s11527-018-1291-z.

[171] R. Gettu, A. Patel, V. Rathi, S. Prakasan, A.S. Basavaraj, S. Palaniappan, S. Maity, Influence of supplementary cementitious materials on the sustainability parameters of cements and concretes in the Indian context, Mater. Struct. 52 (2019) 1–11, https://doi.org/10.1617/s11527-019-1321-5.

[172] https://www.ecoinvent.org/database/older-versions/ecoinvent-33/ecoinvent-33.htmlEcoinvent database.

[173] L.K. Turner, F.G. Collins, Carbon dioxide equivalent (CO2-e) emissions: a comparison between geopolymer and OPC cement concrete, Construct. Build. Mater. 43 (2013) 125–130, https://doi.org/10.1016/j.conbuildmat.2013.01.023.

[174] K.H. Yang, J.K. Song, K.I. Song, Assessment of CO2 reduction of alkali-activated concrete, J. Clean. Prod. 39 (2013) 265–272, https://doi.org/10.1016/j.jclepro.2012.08.001.

[175] M. Fawer, M. Concannon, W. Rieber, Life cycle inventories for the production of sodium silicates, Int. J. Life Cycle Assess. 4 (4) (1999) 207–212.

[176] R. Gettu, A.S. Basavaraj, Life cycle assessment of LC3: parameters and prognoses, in: Shashank Bishnoi (Ed.), Calcined Clays for Sustainable Concrete, 2020, pp. 28–277.

[177] C. Kumar, S.C. Yaragal, B.B. Das, Ferrochrome ash–Its usage potential in alkali activated slag mortars, J. Clean. Prod. 257 (2020) 120577, https://doi.org/10.1016/j.jclepro.2020.120577.

[178] PRé Consultants, SimaPro LCA software, version 8.0.5.13. www.pre-sustainability.com/simapro. Accessed 17 November 2020.

[179] T. Hanein, J.L. Galvez-Martos, B.M.N. Bannerman, Carbon footprint of calcium sulfoaluminate clinker production, J. Clean. Prod. 172 (2018) 2278–2287, https://doi.org/10.1016/j.jclepro.2017.11.183.

[180] S.C. Paul, Y.W.D. Tay, B. Panda, M.J. Tan, Fresh and hardened properties of 3D printable cementitious materials for building and construction, Arch. Civil Mech. Eng. 18 (2018) 311–319.

[181] M. Sitarz, M. Urban, I. Hager, Rheology and mechanical properties of fly ash-based geopolymer mortars with ground granulated blast furnace slag addition, Energies 13 (10) (2020) 2639, https://doi.org/10.3390/en13102639.